SLAC-PUB-942
(TH) and (EXP)
August 1971

SCALING AND THE BEHAVIOR OF NUCLEON RESONANCES IN INELASTIC ELECTRON-NUCLEON SCATTERING*

E. D. Bloom and F. J. Gilman
Stanford Linear Accelerator Center, Stanford University, Stanford, California 94305

ABSTRACT

The behavior of elastic scattering and of the electroproduction of nucleon resonances is shown to be closely related to the behavior of deep inelastic electron-nucleon scattering. This relation is discussed in the context of duality ideas taken from strong interaction processes. These ideas suggest that a substantial part of the observed behavior of inelastic electron-nucleon scattering is due to a non-diffractive component of virtual photon-nucleon scattering. Through finite energy sum rules quantitative relations between the elastic and resonance electroproduction form factors and the deep inelastic scattering are derived and the behavior of inelastic scattering near threshold is calculated.

(Submitted to Phys. Rev.)

---

* Work supported by the U. S. Atomic Energy Commission.

I. INTRODUCTION

High energy inelastic electron-nucleon scattering is a unique probe of the charge distribution inside the nucleon and provides a method for searching for possible substructure. Since experiments have revealed a large cross section for inelastic electron-proton scattering, there have been many different attempts to understand the physical origin of the observed regularities of the scattering, particularly the deep inelastic scattering at high energies and large momentum transfers. In this paper we will show that the behavior of the deep inelastic scattering is related in a striking way to the behavior of elastic scattering and of nucleon resonance electroproduction. The relation between resonance electroproduction and deep inelastic scattering is tied up closely with theoretical ideas, particularly about duality, which arise from the behavior of purely hadronic scattering processes. This leads us to a discussion of sum rules, and finally to quantitative relations between the elastic and inelastic form factors and the inelastic structure functions. While we have dealt with these questions in a previous short paper[1], we present here an extended discussion of the theoretical ideas as well as their consequences in quantitative detail.

We focus our attention on the process of inelastic electron-nucleon scattering where an electron of known energy (E) is scattered by a nucleon through a measured angle (θ) to a smaller final energy (E') due to the exchange of a single photon.[2] In general the nucleon breaks up due to the scattering and if only the final electron is observed, then the double differential cross section can be written as

$$\frac{d^2\sigma}{d\Omega' dE'} = \frac{4\alpha^2 E'^2}{q^4}\left[2W_1(\nu, q^2)\sin^2\frac{\theta}{2} + W_2(\nu, q^2)\cos^2\frac{\theta}{2}\right] . \qquad (1)$$

The results of the scattering are thus summarized in the structure functions W_1 and W_2 which depend on the exchanged photon's laboratory energy, $\nu = E - E'$, and minus the invariant mass squared, $q^2 = 4EE' \sin^2 \frac{\theta}{2}$. Knowing ν and q^2 from measuring the incident and scattered electron, the invariant mass W of the final hadrons is fixed by

$$s = W^2 = 2M_N \nu + M_N^2 - q^2 . \tag{2}$$

We can also consider inelastic electron scattering as a collision between the exchanged virtual photon and the target nucleon. One is then simply studying the total cross section of the process "γ" + p → hadrons, where the hadrons have an invariant mass W and we are able to vary the energy, mass, and polarization of the incident photon beam. This leads one to define total virtual photon-nucleon cross sections for transversely and longitudinally polarized photons, $\sigma_T(\nu, q^2)$ and $\sigma_S(\nu, q^2)$, which are related to W_1 and W_2 by[2]

$$\begin{aligned} W_1 &= \frac{K}{4\pi^2 \alpha} \sigma_T \\ W_2 &= \frac{K}{4\pi^2 \alpha} \frac{q^2}{q^2 + \nu^2} (\sigma_T + \sigma_S) \end{aligned} \tag{3}$$

where $K = \nu - q^2/2M_N = (W^2 - M_N^2)/(2M_N)$. The longitudinal total cross section σ_S is forced to vanish at $q^2 = 0$ by gauge invariance, while σ_T at $q^2 = 0$ is simply the total photoabsorption cross section (into hadrons) for real photons. By the optical theorem, the total cross section is proportional to the imaginary part of the forward virtual photon-nucleon (or virtual Compton) amplitude. From this viewpoint one regards the two structure functions W_1 and W_2 as two invariant amplitudes in a tensor decomposition[2] of the imaginary part of the virtual Compton

amplitude, and which are therefore linearly related to the total cross sections (by Eq. (3)).

Having established the kinematic framework and notation, we can turn to the physics. In the next section we briefly review the experimental situation for inelastic electron-nucleon scattering and discuss the experimental indications of scaling behavior in deep inelastic scattering. In Section III we turn to the behavior of elastic scattering and of nucleon resonance electroproduction and show that their behavior is closely related to that of the deep inelastic scattering. We then discuss the relation between resonance electroproduction and deep inelastic scattering in the context of duality ideas taken from strong interactions, which suggest that a substantial part of the observed behavior of inelastic electron-nucleon scattering is due to a non-diffractive component of virtual photon-nucleon scattering. This leads in Section IV to a discussion of finite energy sum rules and quantitative relations between the elastic and resonance electroproduction form factors and the inelastic structure functions. In particular, we derive and discuss the behavior of the inelastic scattering near threshold. Finally, a summary and discussion is given in Section V.

II. DEEP INELASTIC SCATTERING EXPERIMENTS AND SCALING

The large cross sections observed for deep inelastic electron-proton scattering[3] have led to descriptions of the scattering in terms of point-like constituents (partons) of the nucleon.[4] In the parton descriptions, both the point-like magnitude of the deep inelastic scattering data and the scaling behavior proposed earlier by Bjorken[5] arise in a natural manner. "Scaling" is the statement that as ν and $q^2 \to \infty$, νW_2 and W_1 become non-trivial functions of the dimensionless ratio

$\omega = 2M_N\nu/q^2$ only, rather than functions of both ν and q^2 separately, as would be the case a priori. Since from a theoretical standpoint scaling is a statement of behavior in the Bjorken limit as ν and $q^2 \to \infty$, any other dimensionless variable ω', such that $\omega' \to \omega$ as ν and $q^2 \to \infty$, is in principle just a suitable as ω for studying the scaling behavior of the experimental data, which exists only at finite values of ν and q^2. Use of another variable, ω', could lead to scaling sooner in the sense that νW_2 and W_1 would become independent of q^2 (and thus equal to their $q^2 \to \infty$ limiting values) if they are studied as functions of q^2 for fixed ω' rather than fixed ω.

This is in fact the case for inelastic electron-proton scattering.[6] If we take the data with $q^2 \geq 1$ GeV^2 and for the moment we stay away from the low W region with prominent nucleon resonances, then there is a more rapid approach to scaling behavior if one uses the variable[6]

$$\omega' = 1 + \frac{W^2}{q^2} = \omega + \frac{M_N^2}{q^2} \quad . \tag{4}$$

Clearly ω' is dimensionless and is the same as ω in the Bjorken limit of ν, $q^2 \to \infty$. There is some indication[7] from inelastic neutrino-nucleon scattering data that scaling also occurs there sooner using ω' rather than ω. Since a best fit[6,8] (in the sense of best scaling behavior) for m^2 in an expression of the form $\omega' = \omega + m^2/q^2$ gives a value of m^2 consistent with M_N^2, and since $\omega' = 1 + W^2/q^2$ is a simple form, we will use ω' as the scaling variable[9,10] in the remainder of this paper.

In order to test for scaling behavior one must separate the contributions of W_1 and W_2 to the double differential cross section in Eq. (1), and then consider

νW_2 and W_1 at fixed ω' and see if they approach limits as q^2 (and ν) $\longrightarrow \infty$. The separation of W_1 and W_2 is accomplished by measuring the scattering at the same value of ν and q^2, but at different angles, and is equivalent to a knowledge of $R = \sigma_S/\sigma_T$. The value of R obtained[8] by averaging over the present data between ω' of 1 and 10 is 0.18 ± 0.10. The values of R do not show any strong dependence on ν, q^2 or ω'. Using a fixed value[11] of R = 0.18, Figure 1 shows νW_2 and $2M_N W_1$ as functions of ω' for various q^2 intervals and $W \geq 2.0$ GeV (beyond the prominent resonances). Both νW_2 and W_1 scale (i.e., are finite and independent of q^2 at fixed ω') to within the accuracy of the data for ω' in the range $1 < \omega' < 10$, as long as $q^2 \geq 1$ GeV^2 and $W \geq 2.0$ GeV.[8]

It will be useful later to have a smooth curve which passes through the data for $\nu W_2(\omega')$. For this purpose we have taken a fit[12] in the form of a polynomial in $(1-1/\omega')$. An excellent fit is obtained with three terms, as

$$\nu W_2(\omega') = 0.557\left(1-\frac{1}{\omega'}\right)^3 + 2.1978\left(1-\frac{1}{\omega'}\right)^4 - 2.5954\left(1-\frac{1}{\omega'}\right)^5 , \qquad (5)$$

and is valid in the range $0.8 > \frac{1}{\omega'} > 0.1$. Figure 2 shows this function and the data for νW_2 assuming R = 0, 0.18, and 0.30 plotted versus $x' = 1/\omega' = q^2/(q^2+W^2)$. We emphasize that we are using this fit as a convenient parametrization of the data only, and it is not to be given any theoretical significance nor to be used outside the range quoted above where it was fit to the data.

From the relation of W_1 and W_2 to the total cross sections σ_S and σ_T in Eq. (3) one expects that as $\omega' \rightarrow \infty$, νW_2 and W_1/ω' go as $(\omega')^{\alpha-1}$, where α is the Regge intercept (at t = 0) of the leading J-plane singularity in forward virtual photon-nucleon scattering. If the leading singularity is that of the Pomeron,

corresponding to diffractive virtual photon-nucleon scattering, then νW_2 and W_1/ω' tend to constants as $\omega' \to \infty$. On the other hand, if a non-diffractive component of forward virtual photon-nucleon scattering is present, then W_2 and W_1/ω' should decrease as $\omega' \to \infty$. Unfortunately, for values of $\omega' > 10$ there is presently no data over a large range of q^2, nor is there a separation of W_1 and W_2. If we use the same (small) value of $R = \sigma_S/\sigma_T$ found for $\omega' < 10$, then the data that are available[3,6] are consistent with scaling behavior and νW_2 decreasing for large values of ω'. In fact, either or both νW_2 and W_1/ω' must decrease by $\sim 20\%$ between their maxima at $\omega' \approx 5$ and $\omega' \approx 25$ if we assume[13] that scaling holds for all ω' as long as $q^2 \geq 1$ GeV^2. This is because for $R = 0$, both νW_2 and W_1/ω' decrease by this amount for large ω' (with the restrictions above), and as we increase the assumed value of R for $\omega' > 10$, the values of νW_2 obtained from the differential cross section measurements go up compared to those obtained assuming $R = 0$, but those of W_1/ω' go down. Since W_1 and νW_2 are now known rather well for $\omega' < 10$, one cannot tamper with W_1 or νW_2 in this region, and therefore one or both must decrease at large ω' as noted above. One may alternately directly consider the values of σ_T at points where a separation has been made. One then finds that at $q^2 = 1.5$ GeV^2, σ_T is a maximum near $\omega' = 4$ and falls with increasing energy at least as much as the total photoabsorption cross section does over the same ν or W^2 range at $q^2 = 0$.[8] Thus, there is experimental evidence[14] from the energy dependence of the measured cross sections for a non-diffractive component to virtual photon-nucleon scattering at values of q^2 for which there is scaling for $\omega' < 10$.

More direct evidence for the presence of an isospin dependent and therefore non-diffractive component of the amplitude is to be found in the difference between

inelastic scattering from protons and neutrons.[6] Neglecting corrections for internal motion, final state interactions, and Glauber corrections, the neutron cross sections are given by the difference of the derterium and hydrogen cross sections.[15] The data indicate that the neutron cross sections are smaller than the proton cross sections over a large kinematic range. In particular, assuming the same value of $R = \sigma_S/\sigma_T$ for the neutron and proton, $\nu W_{2n}/\nu W_{2p}$ is smaller than unity at least for $\omega' \lesssim 6$, and νW_{2n} scales within the accuracy of the data. If one plots $\nu W_{2p} - \nu W_{2n}$, then there appears[6] to be a maximum near $\omega' = 4$, at which point $\nu W_{2p} - \nu W_{2n} \simeq 0.1$ and the ratio $\nu W_{2n}/\nu W_{2p} \approx 2/3$. While the neutrino data may also suggest that the scattering of neutrinos on neutrons and protons is different[7], the electroproduction data is the most direct and conclusive experimental evidence for an isospin dependent, non-diffractive component of the amplitude for forward virtual photon-nucleon scattering.

III. THE BEHAVIOR OF NUCLEON RESONANCE ELECTROPRODUCTION AND DUALITY

A non-diffractive component of a forward amplitude and the corresponding decreasing total cross section at high energy are correlated with the presence and behavior of resonances a low energy, at least for purely hadronic processes.[16] In particular, total cross sections for processes like K^+p and pp scattering, which have no obvious s-channel resonances at low energy, have essentially constant total cross sections above laboratory energies of a few GeV, while processes like K^-p and $\bar{p}p$ scattering, which have many strong s-channel resonances at low energy, have total cross sections which decrease substantially as the energy is increased above a few GeV. This correlation of the behavior of total cross

sections and the presence of resonances is part of the "two component" picture[16] of duality for two body amplitudes. In this picture, "Pomeron exchange" or diffraction at high energies is connected to the low energy non-resonant "background", while "ordinary" exchanges (non-Pomeron Regge trajectories or cuts) are connected to the low energy s-channel resonances. The connection of resonances at low energies to "ordinary" exchanges at high energies takes quantitative form in terms of finite energy sum rules.[17] These sum rules relate integrals over the imaginary part of the amplitude at low energies to the properties (residue functions, Regge trajectories) of the t-channel exchanges at high energies.[18]

Given the presence of a non-diffractive component of the forward virtual photon-nucleon amplitude in the scaling region (from the experimental observations of energy dependence and neutron-proton differences in inelastic electron-nucleon scattering at values of q^2 where scaling is observed), we expect that for $q^2 \gtrsim 1$ GeV^2 nucleon resonance electroproduction will have a behavior which is correlated with other features of deep inelastic scattering. In particular, we would like to compare the behavior of the resonances with the behavior of νW_2 and W_1 in the region where scaling behavior is observed.

The behavior of the resonances in comparison to νW_2 in the scaling limit can be seen from Figures 3 and 4 where we have plotted the function νW_2 versus ω' at various values of q^2 (assuming $R = \sigma_S/\sigma_T = 0.18$). The solid line, which is the same in all cases is the fit[12] described in Section II to the data for $W \geq 1.8$ GeV and $q^2 \geq 1$ GeV^2 where scaling in ω' is observed. We shall call this curve, therefore, the "scaling-limit-curve". The values of νW_2 at fixed q^2 are obtained by interpolating the 6° and 10° data[3] up to a hadron mass, W, of 3 GeV. Above $W \simeq 1.8$ GeV, where there are no prominent resonances visible, the interpolated values

of νW_2 at fixed q^2 agree with the scaling-limit-curve, $\nu W_2(\omega')$, as they should.[12]

We first of all note that we can easily distinctly see the prominent N* resonances at values of q^2 where νW_2 scales for $W \gtrsim 2$ GeV. A given resonance (including the elastic peak) occurs at $\omega'_R = 1 + M_R^2/q^2$ and moves toward $\omega' = 1$ as q^2 increases. We also note that the prominent resonances do not disappear with increasing q^2 relative to a "background" under them which has the scaling behavior. (Note that for values of q^2 beyond about 3 GeV^2 the present data is not of sufficiently high statistical quality in the low W region to reveal whether the prominent resonances are still present.) Instead, the prominent resonances (and the background) seem to roughly follow in magnitude the scaling-limit-curve at the corresponding value of ω'. This can be seen even more clearly in Figures 5, 6, and 7 where the heights of the N*(1238), N*(1520), and N*(1688) nucleon resonance bumps in νW_2 divided by νW_2 ($\omega' = 1 + M_R^2/q^2$) are plotted versus q^2 at points taken from 6° and 10° spectra. The height of the resonance bumps in νW_2 is taken from fits of M. Breidenbach[19] in terms of Breit-Wigner resonance forms and a polynomial background made directly to the measured double differential cross sections. The quantity $\nu W_2(\omega')$ is again the value of the scaling-limit-curve evaluated at a value of ω' which corresponds to the given resonance at the particular value of q^2 measured in the 6° and 10° experiments. Clearly, the ratio of the height of the resonance bump to the magnitude of the scaling-limit-curve remains roughly constant for the prominent N* resonances as q^2 changes from 1 to 3 GeV^2.

Thus at least the prominent nucleon resonances have a behavior which is strongly correlated with the scaling behavior of νW_2. Furthermore, a recent analysis[20] of $R = \sigma_S/\sigma_T$ for $W < 2$ GeV shows the same small value (consistent

with zero) that is found in the scaling region. In addition, we know that elastic scattering is less from neutrons than from protons, just as is the deep inelastic scattering. One, of course, cannot determine without a detailed partial wave analysis what the q^2 dependence is of the many broad, low spin N* resonances that we know exist from pion-nucleon phase shifts. But the behavior of the prominent N* resonances that we can see gives us the clue as to what is happening. We thus propose[1,21] that a substantial part of the scaling behavior of the virtual photon-nucleon amplitude is due to a non-diffractive component of the amplitude. In a duality framework we say that the nucleon and N* resonances at low energy are an intrinsic part of the scaling behavior and correspond to the presence of non-Pomeron exchanges at high energy. The resonances build up, in the sense of finite energy sum rules, the non-diffractive part of the amplitude on the average and yield the non-Pomeron exchanges at high energy, resulting in a falling σ_T or νW_2 (ω') curve at high energies and a difference between neutron and proton inelastic scattering.

Note that neither the decrease of νW_2 or σ_T at high energies, nor the difference between neutron and proton elastic scattering and the similar difference between neutron and proton inelastic scattering, nor the small value of R measured in both the resonance region and deep inelastic scattering, nor the presence of prominent resonance bumps in νW_2 for values of q^2 where scaling holds above $W \simeq 2.0$ GeV, nor even the survival of the prominent resonances relative to "background" depend on using the variable ω'. All of these important aspects of the physics which are basic to our arguments can be seen when we look at the data when plotted with respect to other variables like ω. In some ways the particular choice of variable is similar to the situation in the choice of ν_{lab} or s in

extrapolating high energy fits or models of pion-nucleon charge exchange into the low energy region. While extrapolation with some variables results in better averaging of the resonance region, the essential physics, which was the impetus for much of the original thinking about duality, does not change, e.g., the correlation between zeroes in the angular distributions of the prominent resonances and the zeroes at fixed t in the high energy spin flip and spin nonflip amplitudes.[17] Similarly in electroproduction, much of the physics does not depend on ω'.

That is not to say that ω' does not have advantages. First, as we saw in Section II, scaling occurs earlier in ω'. Second, if νW_2 is considered as a function of ω, the nucleon pole term in νW_2, corresponding to elastic scattering, always occurs at $\omega = 1$. All the other resonances are at values of $\omega > 1$ and move toward $\omega = 1$ as q^2 increases. Using $\omega' = 1 + W^2/q^2$, however, the nucleon and all other resonances occur at values of $\omega' > 1$. The nucleon is then not treated in a special way compared to the other resonances. As we will see in the next section, this allows one to understand in an alternate way the connection found previously between the behavior of the elastic form factors and of νW_2 as $\omega' \longrightarrow 1$. Third, the use of ω' allows a much more local averaging of the region below $W \simeq 2$ GeV where there are prominent resonances.

What is unique to studying duality in electroproduction is of course the experimentally observed scaling behavior. This allows one to consider data at fixed values of ω', but different values of q^2 and W^2, both within and outside the region of prominent resonances. Thus we can compare the <u>data</u> where there are prominent narrow resonances directly with <u>data</u> for $\nu W_2(\omega')$ for large q^2 and W^2 where nature has accomplished the appropriate averaging of the many broad

resonances and background or t-channel exchanges present there. Hence, without any extrapolation to low energies using a model or theory valid in the high energy region, one can directly see the beautiful oscillations of W_2 in the low W region about the scaling limit curve, which represents the average of many resonances and background at large W. We will give this comparison quantitative form in terms of finite energy sum rules in the next section.

IV. FINITE ENERGY SUM RULES FOR ELECTROPRODUCTION STRUCTURE FUNCTIONS

The possibility of making a quantitative connection using finite energy sum rules between the low W region where there is N* resonance excitation and the deep inelastic region where scaling takes place is already suggested by Figs. 3 and 4 where the scaling-limit-curve appears to roughly average the resonances in νW_2. To derive the relevant sum rule let us consider a fixed value of $q^2 \geq 1$ GeV^2, where νW_2 and W_1 exhibit scaling in ω' to within the accuracy of the data if the hadron mass W is outside the region of the prominent resonances, i.e., $W \gtrsim 2$ GeV. The usual derivation of a finite energy sum rule[17] proceeds by forming the difference of $\nu W_2(\nu, q^2)$ and the leading terms in its high energy behavior, which we choose to parametrize in the Regge form, $\sum_i c_i(q^2)(\omega')^{\alpha_i(0)-1}$. We need only consider here the terms with Regge intercepts $\alpha_i(0) > 0$, which conventionally are taken to be those due to the Pomeron with $\alpha(0) = 1$ and to the P' and A_2 with $\alpha(0) \simeq \frac{1}{2}$. If we then consider the amplitude whose imaginary part is $\nu W_2(\nu, q^2) - \sum_i c_i(q^2)(\omega')^{\alpha_i(0)-1}$, it vanishes faster than $1/\nu$ as $\nu \to \infty$ and, neglecting a possible real term with $\alpha(0) = 0$, we have a superconvergence relation[22],

$$\int_0^\infty d\nu \left[\nu W_2(\nu, q^2) - \sum_i c_i(q^2)(\omega')^{\alpha_i(0)-1} \right] = 0.$$

In the limit where $q^2 \to \infty$, this superconvergence relation multiplied by $2M_N/q^2$ becomes

$$\int_1^\infty d\omega' \left[\nu W_2(\omega') - \sum_i c_i(\infty)\omega'^{\alpha_i(0)-1} \right] = 0$$

since $\nu W_2(\nu, q^2) \to \nu W_2(\omega')$ as $q^2 \to \infty$. If, for some fixed value of q^2, we multiply the first relation by $2M_N/q^2$ and subtract the second with $\omega' = (2M_N\nu + M_N^2)/q^2 = 1 + W^2/q^2$, we obtain

$$\frac{2M_N}{q^2} \int_0^\infty d\nu \left[\nu W_2(\nu, q^2) - \nu W_2(\omega') - \sum_i \left(c_i(q^2) - c_i(\infty) \right) \omega'^{\alpha_i(0)-1} \right]$$
$$= \int_1^\infty d\omega' \left[\nu W_2(\nu, q^2) - \nu W_2(\omega') - \sum_i \left(c_i(q^2) - c_i(\infty) \right) \omega'^{\alpha_i(0)-1} \right] = 0 . \quad (6)$$

To obtain Eq. (6) we must assume that a possible extra real term (a term with $\alpha(0) = 0$) in the high energy forward virtual photon-nucleon amplitude either is absent or is the same[23] in the amplitudes corresponding to $\nu W_2(\nu, q^2)$ and $\nu W_2(\omega')$. Introduction of extra real terms which are not the same in both amplitudes results in the replacement of the zero on the right hand side of Eq. (6) with an arbitrary function of q^2. The success of the sum rule in Eq. (7) below can then be taken as a posteriori evidence against the presence of different extra real terms in the high energy behavior of the amplitudes corresponding to $\nu W_2(\nu, q^2)$ and $\nu W_2(\omega')$.

Above some sufficiently large value of $\nu = \nu_R$ (and corresponding value of $\omega' = \omega'_R$) the functions $\nu W_2(\nu, q^2)$ and $\nu W_2(\omega')$ must agree with the leading terms

in their asymptotic behavior to any desired accuracy. The upper limit in the integral in Eq. (6) may then be changed to ν_R (or ω'_R). Furthermore, we recall that to within the accuracy of the data we have scaling in ω' for $q^2 \geq 1$ GeV^2 and values of ν greater than $\nu_m = (W_m^2 - M_N^2 + q^2)/(2M_N)$, where W_m is a hadron mass $\simeq 2$ GeV. Thus empirically, the quantities $|\nu W_2(\nu, q^2) - \nu W_2(\omega')|/\nu W_2(\omega')$ and $|c_i(q^2) - c_i(\infty)|/c_i(\infty)$ are consistent with being $<< 1$ for $\nu > \nu_m$. We assume that this is in fact the case. Then the upper limit on the integral in Eq. (6) can be lowered still further to ν_m (or $\omega' = 1 + W_m^2/q^2$), and we can rewrite Eq. (6) as the following sum rule:

$$\frac{2M_N}{q^2}\int_0^{\nu_m} d\nu\ \nu W_2(\nu, q^2) = \int_1^{1+W_m^2/q^2} d\omega'\ \nu W_2(\omega')\ . \tag{7}$$

In comparison to the usual finite energy sum rules[17], Eq. (7) appears very similar except that the usual sum over Regge terms on the right hand side has effectively been replaced by $\nu W_2(\omega')$, which contains the relevant information on high energy behavior. In the present case we do not need to extrapolate a high energy Regge expansion to threshold. We will in fact use Eq. (7) in regions where an expansion in terms of a few powers of ν or ω' is out of the question. Because we can vary the external photon mass in electroproduction and have scaling, we can directly measure a smooth curve which averages the resonances in the sense of finite energy sum rules.

We have tested the validity of the sum rule in Eq. (7) by using the interpolations of $\nu W_2(\nu, q^2)$ to fixed q^2 (shown in Figs. 3 and 4) for the integrand on the left-hand side, and the scaling-limit-curve[12] of Eq. (5) for $\nu W_2(\omega')$ on the right-hand side. The results for the value of $W_m = 2.0$ GeV is shown in Table I for values of q^2 from 1.0 GeV^2 up to 3.0 GeV^2. The agreement of the two sides of Eq. (7) is on the order of 10% or better over the whole range of values of q^2 while each side is changing by about an order of magnitude. Changing R from 0.18 to zero leads to slightly better agreement.[25] Considering the statistical as well as systematic errors present in both the data and the interpolation to fixed q^2, the

agreement is extremely good. Furthermore, the removal of the prominent resonance contributions to $\nu W_2(\nu, q^2)$ would destroy this agreement, the elastic contribution alone being roughly 10% of the integral on the left-hand side. Thus, at least in the region of q^2 where there are still prominent resonance peaks visible the two sides of Eq. (7) agree, and the resonance contributions are a significant part of that agreement. In Fig. 8 the difference of the two sides of Eq. (7), $I_R - I_L$, divided by I_R are shown for $q^2 = 1.0$, 2.0, and 3.0 GeV^2 as functions of the cut-off, W_m. The figure indicates that the sum rule is in fact well satisfied for values of W_m considerably below 2 GeV.

The success of the sum rule in Eq. (7) leads one to investigate whether a more local version of the sum rule could also be true. Specifically, if we form the difference between two versions of Eq. (7) with different upper limits of integration, we obtain

$$\frac{2M_N}{q^2} \int_{\nu_a}^{\nu_b} d\nu\, \nu W_2(\nu, q^2) = \int_{1+W_a^2/q^2}^{1+W_b^2/q^2} d\omega'\, \nu W_2(\omega') \quad , \tag{8}$$

where $\nu_a = (W_a^2 - M_N^2 + q^2)/(2\,M_N)$ and $\nu_b = (W_b^2 - M_N^2 + q^2)/(2M_N)$ correspond to W_a and W_b respectively. If both W_a and W_b are greater than about 2 GeV then Eq. (8) will be satisfied because of the scaling of νW_2. Eq. (8) then becomes interesting only if the masses W_a and W_b are in the low energy region of prominent resonances. To test Eq. (8), we have again used the interpolations to fixed q^2 for νW_2 (shown in Figs. 3 and 4) and the scaling-limit-curve of Eq. (5) for $\nu W_2(\omega')$, and have somewhat arbitrarily chosen the limits on the integrals to correspond to the region of the nucleon and first resonance ($W_a = 0$, $W_b = 1.4$ GeV); the second resonance ($W_a = 1.4$ GeV, $W_b = 1.6$ GeV); the third resonance ($W_a = 1.6$ GeV, $W_b = 1.8$ GeV); and the fourth resonance ($W_a = 1.8$ GeV, $W_b = 2.0$ GeV). The

results are presented in Tables II, III, IV, and V, and show agreement between the two sides of Eq. (8) to 20% or better over the range 1 GeV$^2 \leq q^2 \leq$ 3 GeV^2 with the limits of integration given above.

The success of the sum rules in Eqs. (7) and (8) and the behavior of the prominent resonances in Figs. 5, 6, and 7 in "following" $\nu W_2(\omega')$ is at first surprising if one thinks of the deep inelastic scattering as being characterized by a cross section with a slow falloff in q^2, while elastic scattering and N* electroproduction fall rapidly with increasing q^2. That there is no contradiction here is shown in Fig. 9 where the experimentally measured combination of total cross sections, $\sigma_T + \epsilon\sigma_S$, is plotted against q^2/W^2 for various hadron masses W. Also shown is $G_E^2(q^2) + (q^2/4M_N^2)\ G_M^2(q^2)$, the analogue of $\sigma_T + \sigma_S$ for W = 0.94 GeV, i.e., elastic scattering. Notice in particular the slow (like $1/q^2$) falloff of $\sigma_T + \epsilon\sigma_S$ when $1/9 < q^2/W^2 < 1/3$ corresponding to the relatively flat part of νW_2 between ω' of 4 and 10 in Fig. 1. But when q^2/W^2 becomes large we come below the knee in νW_2 and $\sigma_T + \epsilon\sigma_S$ falls rapidly, roughly like $1/q^6$ for fixed W. From Eq. (3), a $1/q^6$ behavior for $\sigma_T + \sigma_S$ as $q^2 \longrightarrow \infty$ implies that[8]

$$\nu W_2 \propto (W^2/q^2)^3 = (\omega' - 1)^3 \tag{9}$$

as $q^2/W^2 \longrightarrow \infty$ or $\omega' \longrightarrow 1$. The behavior $\sigma_T + \sigma_S \propto 1/q^6$ as $q^2 \longrightarrow \infty$ at fixed W is of course just the behavior of the elastic analogue of $\sigma_T + \sigma_S$, $G_E^2(q^2) + (q^2/4M_N^2)\ G_M^2(q^2)$, at large q^2 if we take dipole forms for $G_{Ep}(q^2)$ and $G_{Mp}(q^2)$. As noted many times previously, the deep inelastic (W > 2 GeV) cross section does fall with increasing q^2 more slowly than elastic scattering at the same value of q^2, particularly for values of q^2 of a few GeV^2 for which ω' is in the range where νW_2 is approximately constant. But for sufficiently large values of q^2 the cross section for any fixed W falls rapidly, very much as elastic scattering does already at much lower values of q^2.

What then must be the large q^2 behavior of the form factor of a given hadronic final state of mass W if it is to participate in the scaling behavior of νW_2? It is rather simple to show[1] that if $G(q^2)$ is the excitation form factor[26] of the hadronic final state of mass W and

$$G(q^2) \longrightarrow c\left(\frac{1}{q^2}\right)^{n/2} \tag{10}$$

as $q^2 \longrightarrow \infty$, and if νW_2 can be parametrized as

$$\nu W_2 \longrightarrow c' \, (\omega' - 1)^p \tag{11}$$

as $\omega' \longrightarrow 1$, then these two behaviors can coexist only if

$$n = p + 1. \tag{12}$$

Thus each hadronic final state of mass W, if it is to participate in the scaling behavior, must have an excitation form factor with a specific power of falloff in q^2 as $q^2 \longrightarrow \infty$, and this power is the same for all W and is related to the power with which νW_2 rises at threshold. If we apply this in the low energy region to a given resonance of mass W_R, then all resonances which follow $\nu W_2(\omega')$ in magnitude (as we have seen the prominent N* resonances do) must have the same power of falloff in q^2 as $q^2 \longrightarrow \infty$ (including presumably the zeroeth resonance or elastic contribution to νW_2 which has $n \simeq 4$), and again this is related to the behavior of νW_2 at threshold. That the resonance excitation form factors all have a behavior at large q^2 which is similar to the behavior of the elastic form factor (with $n \simeq 4$) has been previously indicated.[6,27] As we have $p \simeq 3$ from Eq. (9), it also follows that Eq. (12) is at least approximately satisfied. For the case of the elastic peak in νW_2, Eq. (12) is just the relation of Drell and Yan[27] first found in the parton model. Clearly, in deriving Eq. (12) we did not need or predict the magnitude of the coefficients in Eqs. (10) and (11).

One should note, however, that the larger the mass of the resonance or hadronic state, the larger must be the value of q^2 to be in the region of $\omega' = 1 + W^2/q^2$ near 1 where the behavior expressed in Eq. (12) holds. Said in another way, if we now parameterize all resonance form factors at large q^2 as dipoles, the mass appearing in the dipole expression will increase as the mass of the resonance increases.[29]

The possibility, suggested by Figs. 5, 6, and 7, that the scaling behavior is reflected in the resonances on an almost resonance by resonance basis leads us to try taking the finite energy rum rule average over very local regions of W. Consider, for example, the region of ω' from $\omega' = 1$ to an ω' corresponding approximately to the threshold for single pion electroproduction. This is the one region of ω' where we know exactly what resonances are present and their quantitative contribution to the sum rules--only the elastic delta function in $\nu W_2(\nu, q^2)$ makes a contribution to the left-hand side of Eq. (7) or (8). It is very instructive to carry the assumption of local duality to an extreme and assume that the area (in the sense of the left-hand side of Eq. (7)) under the elastic peak in νW_2 for large q^2 is also the same as the area (in the sense of the right-hand side of Eq. (7)) under the scaling-limit-curve between $\omega' = 1$ and a value of ω' corresponding to a hadron mass W_t around physical pion threshold, i.e.,

$$\int_1^{1+W_t^2/q^2} d\omega' \; \nu W_2(\omega') = \frac{2M}{q^2} \int d\nu \; \nu W_2^{\text{elastic}}(\nu, q^2)$$

$$= \left[G(q^2)\right]^2 = \left[F_1(q^2)\right]^2 + \frac{q^2 \mu_A^2}{4M_N^2}\left[F_2(q^2)\right]^2$$

$$= \frac{\left[G_E(q^2)\right]^2 + \frac{q^2}{4M_N^2}\left[G_M(q^2)\right]^2}{1 + q^2/4M_N^2} \; .$$

Taking the derivative of this equation with respect to q^2, we obtain

$$\nu W_2\left(\omega' = 1 + \frac{W_t^2}{q^2}\right) = \frac{1}{\omega' - 1}\left(-q^2 \frac{d}{dq^2}\left[G(q^2)\right]^2\right), \tag{14}$$

which allows us to calculate $\nu W_2(\omega')$ near threshold in terms of the elastic form factors once we have chosen W_t.

However, note that no matter what value we choose for W_t we again obtain the relation of Eq. (12) between the behavior of the elastic form factor at large q^2 and the threshold behavior of $\nu W_2(\omega')$. For if $G(q^2) \to (1/q^2)^{n/2}$ as $q^2 \to \infty$, and $\nu W_2(\omega') \to (\omega' - 1)^p$ as $\omega' \to 1$, then Eq. (14) demands that $n = p + 1$, as before. Furthermore, by comparing Eq. (14) for neutrons and protons, using the same value of W_t, one obtains[30]

$$\frac{W_{2n}}{W_{2p}} = \frac{-q^2 \frac{d}{dq^2}\left[G_n(q^2)\right]^2}{-q^2 \frac{d}{dq^2}\left[G_p(q^2)\right]^2} \xrightarrow[q^2 \to \infty]{\omega' \to 1} (\mu_n/\mu_p)^2 = .47. \tag{15}$$

Ignoring deuterium corrections[15], this is in agreement with at least the trend of the present data[6] (which only extend down to $\omega' \simeq 1.7$). Finally, if we apply the same assumptions of elastic dominance in a finite energy sum rule for W_1, we obtain[31]

$$R = \sigma_S/\sigma_T \xrightarrow[q^2 \to \infty]{\omega' \to 1} 0, \tag{16}$$

which is again quite consistent with experiment.[8]

While these semiquantitative results are all in rough agreement with present experimental results, a more quantitative investigation of Eq. (14) reveals some difficulties. In particular, using parametrizations of the measured proton form factors[32], we have used Eq. (14) to calculate $\nu W_2(\omega')$ for various choices of W_t. We should only expect the very strong assumptions made in deriving Eq. (14) to work when scaling in ω' holds and when the elastic peak is pushed into the threshold region of $\nu W_2(\omega')$, i.e., when $q^2 \gg 1$ GeV^2 and $\omega' - 1 = (W_t^2/q^2) \ll 1$. The results of the calculation[32] are shown in Figure 10 for two values of W_t together with the available large angle data points[8] near $\omega' = 1$. Although the correct shape of $\nu W_2(\omega')$ for $\omega' - 1 \lesssim 0.5$ is obtained when $W_t = 1.08$ GeV, corresponding to physical pion threshold, the resulting curve is too high by a factor of 2 to 3. To obtain a calculated curve which passes through the data below $\omega' = 1.5$ one must use a value of $W_t \simeq 1.23$ GeV, corresponding to an energy just below the peak of the first resonance. Stated another way, the elastic contribution to the left-hand side of Eq. (7) equals the area under $\nu W_2(\omega')$ from $\omega' = 1$ all the way up to an ω' which corresponds to a hadron mass just below the peak of the first resonance. The proton pole is doing more than its share in satisfying the sum rule in Eq. (7) at high q^2.

In the calculation of νW_{2p} from the elastic form factors using Eq. (14) one is actually hampered by the lack of knowledge[32] of $G_E(q^2)$ at large q^2. The lack of knowledge of the elastic form factors hampers even more the calculation of $\nu W_{2n}(\omega')$ which may be obtained from the analogue of Eq. (14) for the neutron, but turns out to depend rather strongly on exactly what we choose for the neutron electric form factor. In Figure 11 we have plotted the ratio of νW_2 for the neutron to that of the proton obtained from Eq. (14) for $W_t = 1.23$ GeV and two possible

neutron electric form factors.[32] While both results agree with Eq. (15) in the limit where $\omega' \to 1$, there are strong differences for $\omega' > 1$, representative of effects depending on what the neutron electric form factor does at large q^2 in comparison to the proton form factors and to the neutron magnetic form factor. Hence, surprisingly, the calculation of the inelastic structure functions through Eq. (14) presently runs into difficulties because of lack of knowlege of elastic scattering.

Quite apart from these difficulties in practice, there are also those of principle. In deriving Eq. (14) we have carried the ideas of duality to the extreme point of using local averaging (in the sum rule sense) over a single infinitely narrow resonance, the nucleon. That this should work even qualitatively is surprising. But why not apply the same local averaging to, say, the first resonance, which, while giving the Drell-Yan relation and Eq. (16) for R, would predict from isospin invariance equal scattering from the neutron and proton instead of Eq. (15)? The only objection to this is that in practice the nucleon pole is the only place where we know exactly what resonances are present; at the first resonance there is already a considerable non-resonant amplitude. While the non-resonant amplitude (mostly due to s-wave pion production) is also roughly the same for neutrons and protons in photoproduction, the situation for large q^2 electroproduction is unknown at yet. It will clearly be quite interesting to have data on the neutron elastic and resonance excitation form factors for $q^2 \gtrsim 1$ GeV^2 to compare with the deep inelastic electron-neutron data in the scaling region. We suspect that neutron and proton inelastic scattering for hadrons masses in the first resonance region are roughly equal, even at large q^2. If this is the case then one will have to abandon extreme local averaging, and regard it as illustrative

only. One must then average over larger W regions and include, for example, at least the nucleon and first resonance region in the left-hand side of Eq. (7) or (8) to obtain agreement with the right-hand side. However, we may yet find ourselves in the embarrassing position of having the predictions of Eq. (15) and (16) found to be true experimentally at values of ω' away from 1 where the elastic form factors and Eq. (14) predict deviations from the asymptotic ($\omega' \to 1$) behavior.

Up to this point we have considered only sum rules for νW_2 in detail. Similar considerations could be applied to W_1. However, a knowledge of $R = \sigma_S/\sigma_T$ allows one to calculate W_1 from νW_2 through Eq. (3), and so finite energy sum rules for W_1 are essentially equivalent to those for νW_2 plus a knowledge of $R(\nu, q^2)$. Although detailed knowledge of R is not extant, we know that it is quite small, both in the region of prominent resonances[20] and in the deep inelastic region.[8] The functions νW_2 and W_1 are thus closely related quantities, and it is easy to show that for a (small) constant value of R the lowest moment finite energy sum rule for W_1 is simply a linear combination of the zeroth moment Eq. (7) and second moment sum rules for νW_2. We have explicitly checked the second moment sum rule of νW_2 and found that it is somewhat better satisfied than the zeroth moment sum rule for $W_m \lesssim 2$ GeV and $R = 0.18$, with $|I_R \sim I_L|/I_R \lesssim 7\%$ at $W_m = 2$ GeV, q^2 between 1 and 3 GeV^2, versus 10% for Eq. (7). Hence, the sum rules for W_1 and νW_2 seem to be equivalently satisfied given that R is small.

V. DISCUSSION AND SUMMARY

Similar considerations to those we have been discussing can of course be applied to inelastic neutrino scattering. In this case both vector and axial-vector currents contribute and there are three structure functions,[34] W_1, W_2 and W_3. The parts of W_1 and W_2 due to the weak vector current are related by the conserved vector current hypothesis to the isovector parts of the corresponding electromagnetic structure functions.

Unfortunately, the experimental information necessary to make any comparisons of the resonance and deep inelastic regions for the structure functions of inelastic neutrino scattering is lacking at present. It is interesting to note though, that if we expect the deep inelastic contributions of the vector and axial-vector currents to νW_2 for inelastic neutrino-nucleon scattering to be equal,[34] and we apply the observations and arguments of this paper to the vector and axial-vector currents separately, then the axial vector form factor, $g_A(q^2)$, of the nucleon and those of the nucleon resonances should all fall-off at large q^2 approximately as $1/q^4$, and the axial vector contribution to νW_2 should behave as $(\omega' - 1)^3$ near $\omega' = 1$. Indeed, if we were to apply extreme local duality to the region around the nucleon pole as in Section IV, equal vector and axial-vector contributions to νW_2 would imply that at large q^2

$$g_A(q^2)^2 \simeq \frac{\left[G_E(q^2)\right]^2 + \frac{q^2}{4M^2}\left[G_M(q^2)\right]^2}{1 + q^2/4M_N^2}$$

where $G_E(q^2)$ and $G_M(q^2)$ are the form factors of the isovector component of the vector current ($G_E(0) = 1$, $G_M(0) = 4.7$).

More generally, given information on the axial-vector transitions in the resonance region (up to $W \simeq 2$ GeV), it should be possible to calculate the structure functions in the deep inelastic region using the analogues of Eq. (7). Also, given that a substantial nondiffractive component is present in the scattering, one expects that at least below $\omega' \simeq 5$, neutrino and antineutrino inelastic scattering will be quite different, and νW_3 for inelastic neutrino and antineutrino scattering will be appreciable compared to W_1.

In summary, we have concentrated in this paper on the relation of N* resonance electroproduction to that of deep inelastic electron-nucleon scattering, and discussed this relation in the context of duality. We have found that both qualitatively and quantitatively the behavior of the resonances is remarkably correlated with the scaling behavior of deep inelastic scattering. In particular, as q^2 changes, the prominent N* resonance bumps in νW_2 closely follow the magnitude of the scaling-limit-curve at the corresponding value of the scaling variable ω'. This leads to relations between the behavior of the resonance excitation or elastic form factors at large q^2 and the behavior of $\nu W_2(\omega')$ as $\omega' \to 1$.

A quantitative connection between resonance electroproduction and scaling behavior has been made in terms of finite energy sum rules. When integrated over the region of the prominent N* resonances (up to $W_m \simeq 2$ GeV) the sum rule in Eq. (7) is satisfied to within 10% or better, which is within the statistical and systematic errors inherent in the data and its interpolation to fixed q^2. This led us to consider asking the sum rule average over regions of W of order a few hundred MeV. As an illustration, we applied the idea of extreme local averaging to the region around the elastic peak, and obtained an equation directly relating the values of $\nu W_2(\omega')$ near $\omega' = 1$ to the nucleon's elastic form factors and the

upper limit of final hadron mass, W_t, to which the integral in the sum rule is carried. While a number of semi-quantitative results which roughly agree with experiment near $\omega' = 1$ follow from this, a large value of W_t must be used to obtain good agreement with the deep inelastic electron-proton data near $\omega' = 1$. Also, there are difficulties in principle with the approximation of keeping only one s-channel resonance in the sum rule. Still, given the extreme assumptions necessary to obtain this result, even qualitative agreement with experiment is surprising.

The connection to ideas of duality taken from purely strong interaction processes is very close and interesting. Qualitatively, the correlation between the height of the prominent resonance bumps and the scaling-limit-curve's magnitude, the fact that $R = \sigma_S/\sigma_T$ is small both in the deep inelastic region and in the low energy resonance region, the prediction of neutron-proton differences, etc., provide examples of the correlation between low and high energy phenomena which is at the heart of duality ideas. Quantitatively, the agreement of the finite energy sum rule, Eq. (7), over a large range of q^2 where on can still see that there are resonance bumps present in νW_2 and the averaging of the resonance bumps by the scaling-limit-curve, $\nu W_2(\omega')$, provides a spectacular example of the averaging of resonances to a smooth curve even outside the Regge regime.

The averaging of the resonances by the scaling-limit-curve is exactly the behavior one expects in dual resonance models of electroproduction where the hadronic final state is completely expressible as a sum of resonances. There have been many models of this kind proposed,[35] mostly within the framework of the Veneziano model.[36] Up to now, all such models have been affected with at least one of two diseases[37]: either they have bad asymptotic behavior in ν or q^2, or they lack factorization, which must be a basic property of any model based on resonances.

In addition, many of the models which agree with experiment quantitatively have additional ad hoc assumptions or parameters. Nevertheless, such models are important at least as theoretical laboratories, and show the consistency of scaling with a world made purely out of resonances.

The success of duality ideas in relating the deep inelastic scattering to the resonances in electroproduction opens some interesting questions. In our discussion we have related various properties, particularly those of resonance electroproduction, to the scaling behavior observed to hold for deep inelastic scattering, but we have not predicted scaling. It is tempting to assume a common origin for both properties of electroproduction in terms of point-like substructure within the nucleon, e.g., quark partons which are responsible both for the deep inelastic scattering and for forming N* resonances when they are excited to specific levels. It is difficult to make this into more than a suggestive picture, particularly since one deals with incoherent scattering (the impulse approximation) in the parton model, while resonance phenomena are certainly coherent properties of the whole nucleon. Establishing a connection between the duality approach we have discussed and the point-like constituent approach of the parton model remains an unsolved problem.

What has been shown by the arguments in this paper, by models, and by the experimentally observed difference between deep inelastic electron-proton and electron-neutron scattering is that there is a substantial non-diffractive component present in virtual photon-nucleon scattering at large q^2. Our arguments, though, do not rule out the presence of some diffractive component[14], especially at large ω'. However, the substantial non-diffractive component that we know exists[14], already leads us to expect, as noted before, that at least for $\omega' \lesssim 5$, neutrino and

anti-neutrino scattering will be quite different, that νW_3 will be appreciable compared to W_1, and also that there will be a sizeable spin dependence exhibited if polarized electrons or muons are scattered on a polarized nucleon target. Hopefully, information on these processes as well as further experiments on inelastic electron-nucleon scattering, particularly with observation of some or all the final hadrons, will permit us to extend the nature of the interconnections we have considered in this paper.

ACKNOWLEDGEMENTS

We thank the members of Group A and the theory group at SLAC for helpful discussions. The support of Group A in performing many of the numerical computations is gratefully acknowledged. We also thank H. DeStaebler and J. D. Bjorken for critical comments on the manuscript.

REFERENCES

1. E. D. Bloom and F. J. Gilman, Phys. Rev. Letters 25, 1140 (1970).
2. We use a metric where $q^2 > 0$ corresponds to a space-like four-vector, q_μ. and units where $\hbar = c = 1$. The fine structure constant $\alpha = e^2/4\pi \simeq 1/137$. For a discussion of the kinematics and the relations between the various amplitudes and cross sections see F. J. Gilman, Phys. Rev. 167, 1365 (1968).
3. M. Breidenbach et al., Phys. Rev. Letters 23, 935 (1969); E. D. Bloom et al., Phys. Rev. Letters, 23 , 930 (1969); M. Breidenbach, MIT thesis, 1970, unpublished.
4. J. D. Bjorken, "Current Algebra at Small Distances", Varenna School Lectures, Course XLI, Varenna, Italy (1967); R. P. Feynman, Phys. Rev. Letters 23, 1415 (1969); J. D. Bjorken and E. A. Paschos, Phys. Rev. 185, 1975 (1969).
5. J. D. Bjorken, Phys. Rev. 179, 1547 (1969).
6. E. D. Bloom et al., "Recent Results in Inelastic Electron Scattering", SLAC-PUB-796, report presented to the XVth International Conference on High Energy Physics, Kiev, USSR (1970).
7. G. Myatt and D. H. Perkins, Phys. Letters 34B, 542 (1971); I. Budagov et al., Phys. Letters 30B, 364 (1969).
8. G. Miller et al., SLAC-PUB-815 (1971), unpublished; J. I. Friedman et al., SLAC-PUB-907 (1971), unpublished.
9. Among other possible scaling variables, the "light cone variables" $q_z \pm q = \sqrt{\nu^2 + q^2} \pm \nu$ have been suggested to us by R. P. Feynman (R. P. Feynman, private communication, 1970). The variable $\sqrt{\nu^2 + q^2} - \nu$ is similar to M/ω',

but with m^2 varying from M_N^2 to zero as ω' varies from one to infinity.

10. For other possible variables see V. Rittenberg and H. Rubinstein, Phys. Letters 35B, 50 (1971), and D. Bhaumik and O. W. Greenberg, University of Maryland preprint (1971), unpublished.

11. The validity of scaling for $\omega' < 10$ is independent of the specific value of R assumed as long as it is small.

12. G. Miller, Stanford thesis and SLAC-REPORT-129 (1970), unpublished. This fit was actually made to the large angle data (reference 8) with $W \geq 1.8$ GeV. It is, however, an excellent fit to the small angle data (reference 3) as well, as discussed in Miller's thesis. We have checked that using a fit only to data with $W \geq 2.0$ GeV gives essentially the same results.

13. Note that since we assume scaling holds for all ω' as long as $q^2 \geq 1$, we are effectively assuming that we can interchange the Regge ($\nu \to \infty$, fixed q^2) and Bjorken (ν and $q^2 \to \infty$, ν/q^2 fixed) limits. This is crucial in drawing any conclusion for large ω' at the present time.

14. See the discussion of the relative strengths of the diffractive and non-diffractive parts of the forward virtual Compton amplitude in F. J. Gilman, "Duality and Inelastic Electron-Nucleon Scattering", invited talk presented at the International Conference on Duality and Symmetry in Hadron Physics, Tel-Aviv, Israel, April 5-7, 1971, and SLAC-PUB-896, unpublished, where it is shown that at $\omega' \simeq 5$ at least a quarter of νW_2 is due to the non-diffractive component.

15. The possibility of non-negligible deuterium corrections has been raised by G. West, Stanford University preprint (1971), unpublished, but we doubt that there will be qualitative changes (i. e., that $\nu W_{2n} = \nu W_{2p}$) in the results of reference 6.

16. H. Harari, Phys. Rev. Letters 20, 1395 (1968); P. Freund, Phys. Rev. Letters 20, 235 (1968).

17. R. Dolen, D. Horn, and C. Schmid, Phys. Rev. 166, 1768 (1968).

18. For the odd amplitude in pion-nucleon scattering see reference 17; for the even amplitude see F. J. Gilman, H. Harari, and Y. Zarmi, Phys. Rev. Letters 21, 323 (1968).

19. M. Breidenbach, reference 3.

20. F. W. Brasse et al., DESY preprint (1970), unpublished.

21. In our interpretation of the data for resonance electroproduction and the behavior of νW_2 for large ω' and correspondingly in the proposal of a substantial non-diffractive component of the amplitude for virtual Compton scattering we differ from some previous applications of duality ideas to inelastic electron scattering. See H. Harari, Phys. Rev. Letters 22, 1078 (1969).

22. For an amplitude which is even under crossing (as is the amplitude corresponding to W_2) this is just a standard superconvergence relation; see V. DeAlfaro et al., Phys. Letters 21, 576 (1966). Note that the first contribution to the integral from $\nu W_2(\nu, q^2)$ is from the Born term at $\nu = q^2/2M_N$.

23. In general it is the second of these two possibilities that is the more likely, i.e., the real as well as the imaginary parts of the two amplitudes are the same at high energy. For one, but not the only way this can happen see J. M. Cornwall, D. Corrigan, and R. E. Norton, Phys. Rev. Letters 24, 1171 (1970) and also F. E. Close and J. F. Gunion, SLAC-PUB-892 (1971), unpublished.

24. A previous family of sum rules based on scaling in ω was proposed by H. Leutwyler and J. Stern, Phys. Letters 31B, 458 (1970). See also, V. Rittenberg and H. Rubinstein, reference 10.

25. For a previous evaluation of the sum rule in Eq. (7), commenting on the dependence of $R = \sigma_S/\sigma_T$, see reference 8. Beyond $q^2 \simeq 3$ GeV^2 one cannot definitely see prominent resonant bumps due to the statistical errors in the present data and the interpolation to fixed q^2. However, for $W_m = 2.0$ GeV there is in any case agreement of the two sides of Eq. (7) to better than 10% up to at least $q^2 = 4.5$ GeV^2.

26. $G(q^2)$ is to be regarded as the effective form factor of a hadronic final state of mass W, with a normalization such that for fixed W one has $W_2 \propto [G(q^2)]^2$.

27. See W. K. H. Panofsky in Proceedings of the Fourteenth International Conference on High Energy Physics, Vienna, Austria, 1969 (CERN Scientific Information Service, Geneva, Switzerland, 1969), p. 23, and reference 6.

28. S. D. Drell and T. M. Yan, Phys. Rev. Letters 24, 181 (1970). See also G. West, Phys. Rev. Letters 24, 1206 (1970).

29. See M. Elitzur, Phys. Rev. D3, 2166 (1970), for a discussion of this and other aspects of dipole form factors for the resonance excitations.

30. We are assuming "scaling" of the elastic form factors, $G_{Mp}(q^2)/\mu_p = G_{Mn}(q^2)/\mu_n$; and that $G_{Ep}(q^2)/G_{Mp}(q^2)$ and $G_{En}(q^2)/G_{Mn}(q^2)$ are bounded as $q^2 \to \infty$.

31. This is just the statement that $G_E^2(q^2)/G_M^2(q^2)$ is bounded as $q^2 \to \infty$ so that $\sigma_S/\sigma_T \sim G_E^2(q^2)/\, q^2 G_M^2(q^2) \to 0$ as $q^2 \to \infty$.

32. We have taken $G_{Mp}(q^2)$ from a numerical fit due to G. Miller, reference 12, to the data of D. H. Coward et al., Phys. Rev. Letters 20, 292 (1968) and assumed $G_{Ep}(q^2) = G_{Mp}(q^2)/\mu_p$. If G_{Ep} were set equal to zero, it would lower the calculated curves in Figure 9 by $\approx 10\%$.

33. A review of the recent data on the neutron form factors can be found in R. Wilson, rapporteurs talk at the XVth International Conference on High Energy Physics, Kiev, USSR (1970), published.

34. See J. D. Bjorken and E. A. Paschos, Phys. Rev. D1, 3151 (1970).

35. See, for example, M. Pavkovic, Ann. Phys. (N.Y.) 62, 1 (1971); G. Domokos, S. Kovesi-Domokos, and E. Shonberg, Phys. Rev. D3, 1184 (1971).

36. See M. Bander, Nucl. Phys. B13, 587 (1969); R. Brower and J. H. Weis, Phys. Rev. 188, 2486 (1969); ibid, 188, 2495 (1969); ibid., D3, 451 (1971); P. V. Landshoff and J. C. Polkinghorne, Nucl. Phys. B19, 432 (1970); S. Matsuda and J. T. Manassah, Institute for Advanced Study preprint (1971) unpublished.

37. See the review of M. Ademollo, talk presented at the Symposium on Meson Photo- and Electroproduction at Low and Intermediate Energies, Bonn, September (1970), unpublished.

TABLE I

Values of the left and right hand sides of the sum rule, Eq. (7), for values of q^2 between 1.0 and 3.0 GeV^2, R = 0.18, and for upper limits of the integrands corresponding to $W_m = 2.0$ GeV.

(a)	(b)	(c)	(d)
1.00	0.773	0.863	+ 10.4
1.25	0.551	0.599	+ 8.0
1.50	0.407	0.433	+ 6.0
1.75	0.309	0.322	+ 4.0
2.00	0.239	0.245	+ 2.4
2.25	0.189	0.191	+ 1.0
2.50	0.150	0.150	0.0
2.75	0.122	0.120	- 1.7
3.00	0.0995	0.0973	- 2.3

(a) q^2 (GeV^2)

(b) $I_L = \frac{2M}{q^2} \int_0^{\nu_m} d\nu \; \nu W_2(\nu, q^2)$

(c) $I_R = \int_1^{1+W_m^2/q^2} d\omega' \; \nu W_2(\omega')$

(d) $(I_R - I_L)/I_R$ (%)

TABLE II

Values of the left and right hand sides of the sum rule, Eq. (8), for values of q^2 between 1.0 and 3.0 GeV^2, for R = 0.18, and limits of integration corresponding to the region of the nucleon and first resonance (W_b = 1.4 GeV).

(a)	(b)	(c)	(d)
1.00	0.186	0.235	+ 20.8
1.25	0.122	0.143	+ 14.7
1.50	0.0827	0.0925	+ 10.6
1.75	0.0583	0.0623	+ 6.4
2.00	0.0423	0.0435	+ 2.8
2.25	0.0314	0.0312	- 0.6
2.50	0.0238	0.0230	- 3.5
2.75	0.0187	0.0173	- 8.1
3.00	0.0147	0.0132	- 11.4

(a) q^2 (GeV^2)

(b) $I_L = \frac{2M_N}{q^2} \int_0^{\nu_b} d\nu \; \nu W_2(\nu, q^2)$

(c) $I_R = \int_1^{1+W_b^2/q^2} d\omega' \; \nu W_2(\omega')$

(d) $(I_R - I_L)/I_R$ (%)

TABLE III

Values of the left and right hand sides of the sum rule, Eq. (8), for values of q^2 between 1.0 and 3.0 GeV^2, for R = 0.18, and limits of integration corresponding to the second resonance region ($W_a = 1.4$ GeV, $W_b = 1.6$ GeV).

(a)	(b)	(c)	(d)
1.00	0.144	0.166	+ 13.2
1.25	0.100	0.115	+ 13.0
1.50	0.0722	0.0815	+ 11.4
1.75	0.0537	0.0595	+ 9.7
2.00	0.0410	0.0444	+ 5.4
2.25	0.0320	0.0337	+ 5.0
2.50	0.0264	0.0261	- 1.1
2.75	0.0207	0.0204	- 1.5
3.00	0.0167	0.0162	- 3.1

(a) q^2 (GeV^2)

(b) $I_L = \frac{2M_N}{q^2} \int_{\nu_a}^{\nu_b} d\nu \; \nu W_2(\nu, q^2)$

(c) $I_R = \int_{1+W_a^2/q^2}^{1+W_b^2/q^2} \nu W_2(\omega')$

(d) $(I_R - I_L)/I_R$ (%)

TABLE IV

Values of the left and right hand sides of the sum rule, Eq. (8), for values of q^2 between 1.0 and 3.0 GeV^2, for R = 0.18, and limits of integration corresponding to the third resonance region (W_a = 1.6 GeV, W_b = 1.8 GeV).

(a)	(b)	(c)	(d)
1.00	0.207	0.211	+ 1.9
1.25	0.151	0.153	+ 1.3
1.50	0.113	0.114	+ 1.0
1.75	0.0871	0.0863	- 0.9
2.00	0.0678	0.0667	- 1.6
2.25	0.0537	0.0523	- 2.9
2.50	0.0431	0.0416	- 3.6
2.75	0.0353	0.0334	- 5.7
3.00	0.0292	0.0272	- 7.4

(a) q^2 (GeV^2)

(b) $I_L = \frac{2M_N}{q^2} \int_{\nu_a}^{\nu_b} d\nu \; \nu W_2(\nu, q^2)$

(c) $I_R = \int_{1+W_a^2/q^2}^{1+W_b^2/q^2} d\omega' \; \nu W_2(\omega')$

(d) $(I_R - I_L)/I_R$ (%)

TABLE V

Values of the left and right hand sides of the sum rule, Eq. (8), for values of q^2 between 1.0 and 3.0 GeV^2, for R = 0.18, and limits of integration corresponding to the fourth resonance region (W_a = 1.8 GeV, W_b = 2.0 GeV).

(a)	(b)	(c)	(d)
1.00	0.246	0.250	+ 1.6
1.25	0.179	0.189	+ 5.3
1.50	0.139	0.145	+ 4.1
1.75	0.110	0.114	+ 3.5
2.00	0.0883	0.0908	+ 2.7
2.25	0.0718	0.0732	+ 1.9
2.50	0.0581	0.0596	+ 2.5
2.75	0.0472	0.0491	+ 3.9
3.00	0.0390	0.0407	+ 4.7

(a) $q^2 (GeV^2)$

(b) $I_L = \frac{2M_N}{q^2} \int_{\nu_a}^{\nu_b} d\nu \; \nu W_2(\nu, q^2)$

(c) $I_R = \int_{1+W_a^2/q^2}^{1+W_b^2/q^2} d\omega' \; \nu W_2(\omega')$

(c) $(I_R - I_L)/I_R$ (%)

FIGURE CAPTIONS

Fig. 1 - The functions $2M_N W_1$ and νW_2 plotted versus $\omega' = 1 + W^2/q^2$ for $W \geq 2$ GeV and various q^2 ranges assuming $R = \sigma_S/\sigma_T = 0.18$.

Fig. 2 - The fit (solid line) of G. Miller[12] to νW_2 compared to the large angle data assuming R = 0, 0.18, and 0.3.

Fig. 3 - The function $\nu W_2(\nu, q^2)$ plotted versus $\omega' = 1 + W^2/q^2$ from an interpolation of data to fixed q^2 values of 0.75, 1.00, 1.25, 1.50, and 1.75 GeV^2. The solid line is the scaling-limit-curve, $\nu W_2(\omega')$, a smooth fit[12] to the data in the scaling region. The arrow indicates the position of the elastic peak.

Fig. 4 - Same as Figure 3, but for $q^2 = 2.0$, 2.25, 2.50, 2.75, and 3.0 GeV^2.

Fig. 5 - The ratio of the height of the N*(1238) bump in νW_2 to the value of the scaling-limit-curve, $\nu W_2(\omega')$, at the corresponding value of $\omega' = 1 + M^2_{N*}/q^2$ for values of q^2 between 1.0 and 3.0 GeV^2. Values for the height of the resonance bump are taken from fits to the 6^o and 10^o inelastic spectra by M. Breidenbach.[19] The values of $\nu W_2(\omega')$ are from G. Miller.[12]

Fig. 6 - Same as Figure 5, but for the N*(1520).

Fig. 7 - Same as Figure 5, but for the N*(1688).

Fig. 8 - The difference of the right and left hand sides of Eq. (7), $I_R - I_L$, divided by I_R as a function of the cutoff, W_m, for values of q^2 of 1.0, 2.0, and 3.0 GeV^2.

Fig. 9 - Measured values[3,8] of $\sigma_T + \epsilon \sigma_S$ for various hadron masses, W, plotted versus q^2/W^2. The solid line is $G_{Ep}^2(q^2) + (q^2/4M_N^2)G_{Mp}^2(q^2)$, the elastic analogue of $\sigma_T + \sigma_S$, under the assumption of dipole form factors. Values for the N*(1520) cross section are from M. Breidenbach.[19]

Fig. 10 - Computed values of $\nu W_{2p}(\omega')$ for $W_t = 1.08$ and 1.23 GeV using Eq. (14) and the measured proton elastic form factors. The data points are from reference 8, assuming R = 0.18.

Fig. 11 - Values of $\nu W_{2n}/\nu W_{2p}$ for $W_t = 1.23$ GeV computed using Eq. (14) assuming the magnetic form factors $G_{Mn}(q^2)/G_{Mn}(0) = G_{Mp}(q^2)/G_{Mp}(0)$ and two different assumptions for the neutron electric form factor, $G_{En}(q^2)$. The single data point is from reference 6 and neglects deuterium corrections.

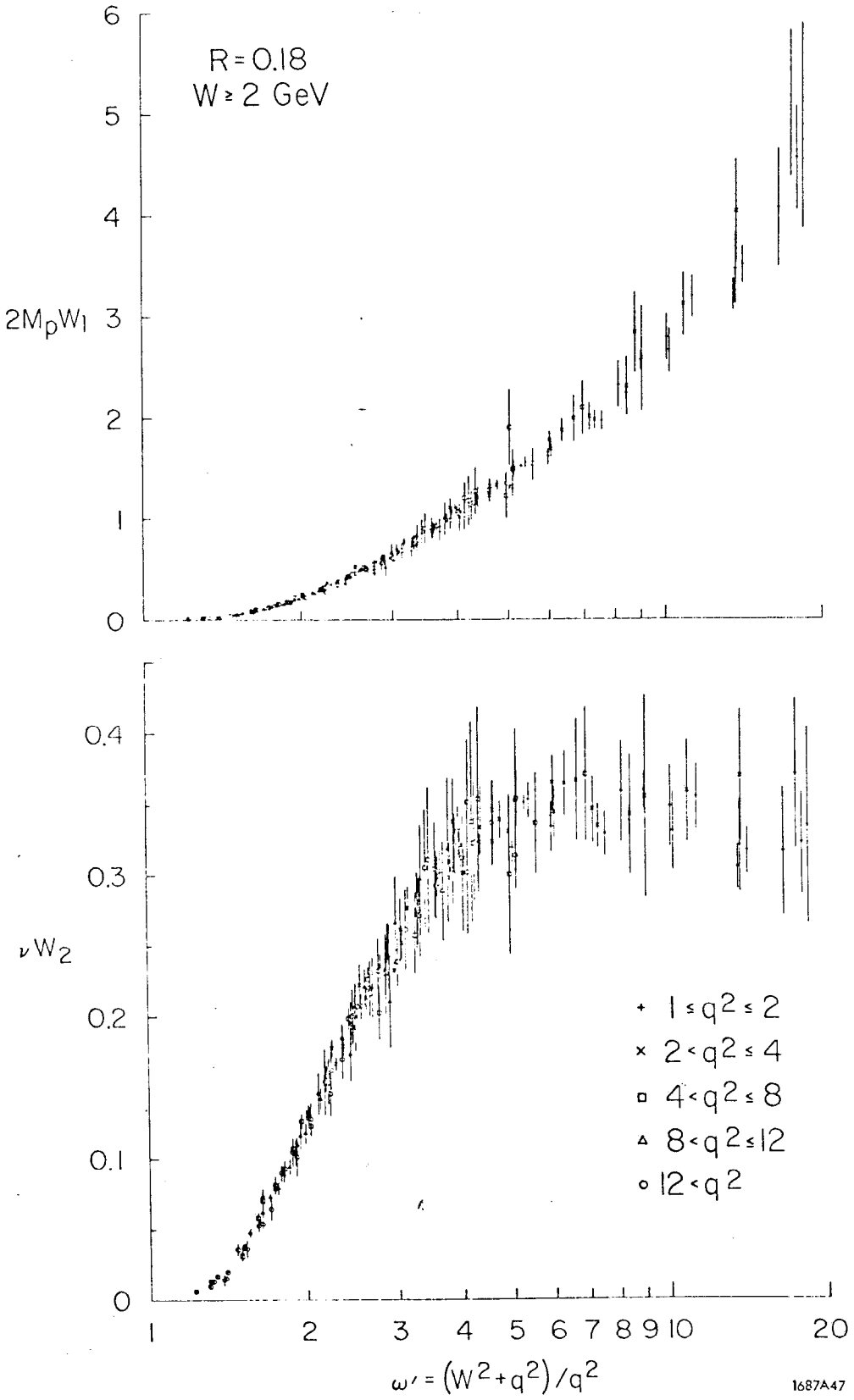
R = 0.18
W ≥ 2 GeV
$2M_pW_1$
νW_2
$1 \le q^2 \le 2$
$2 < q^2 \le 4$
$4 < q^2 \le 8$
$8 < q^2 \le 12$
$12 < q^2$
$\omega' = (W^2+q^2)/q^2$
1687A47

Fig. 1

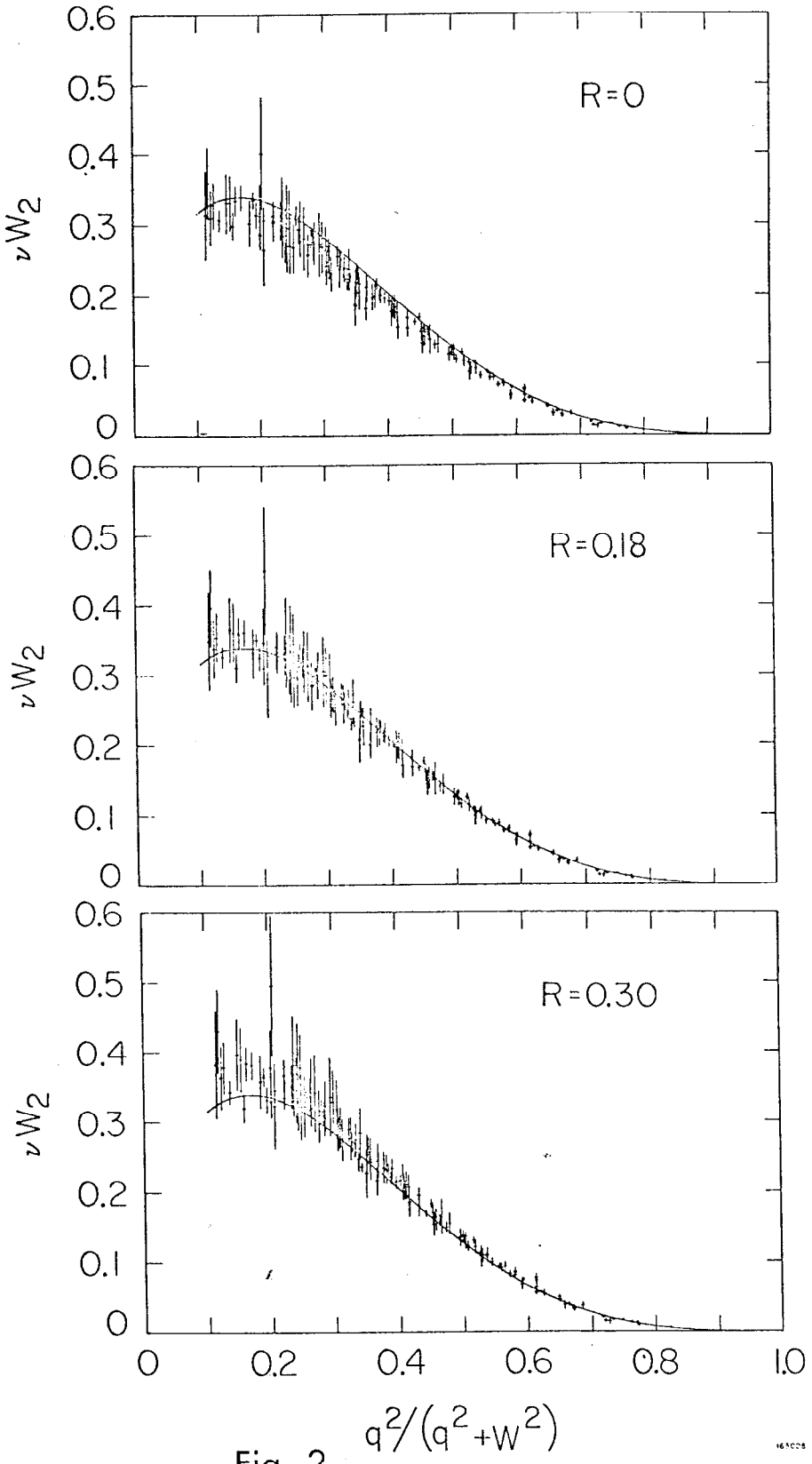

Fig. 2

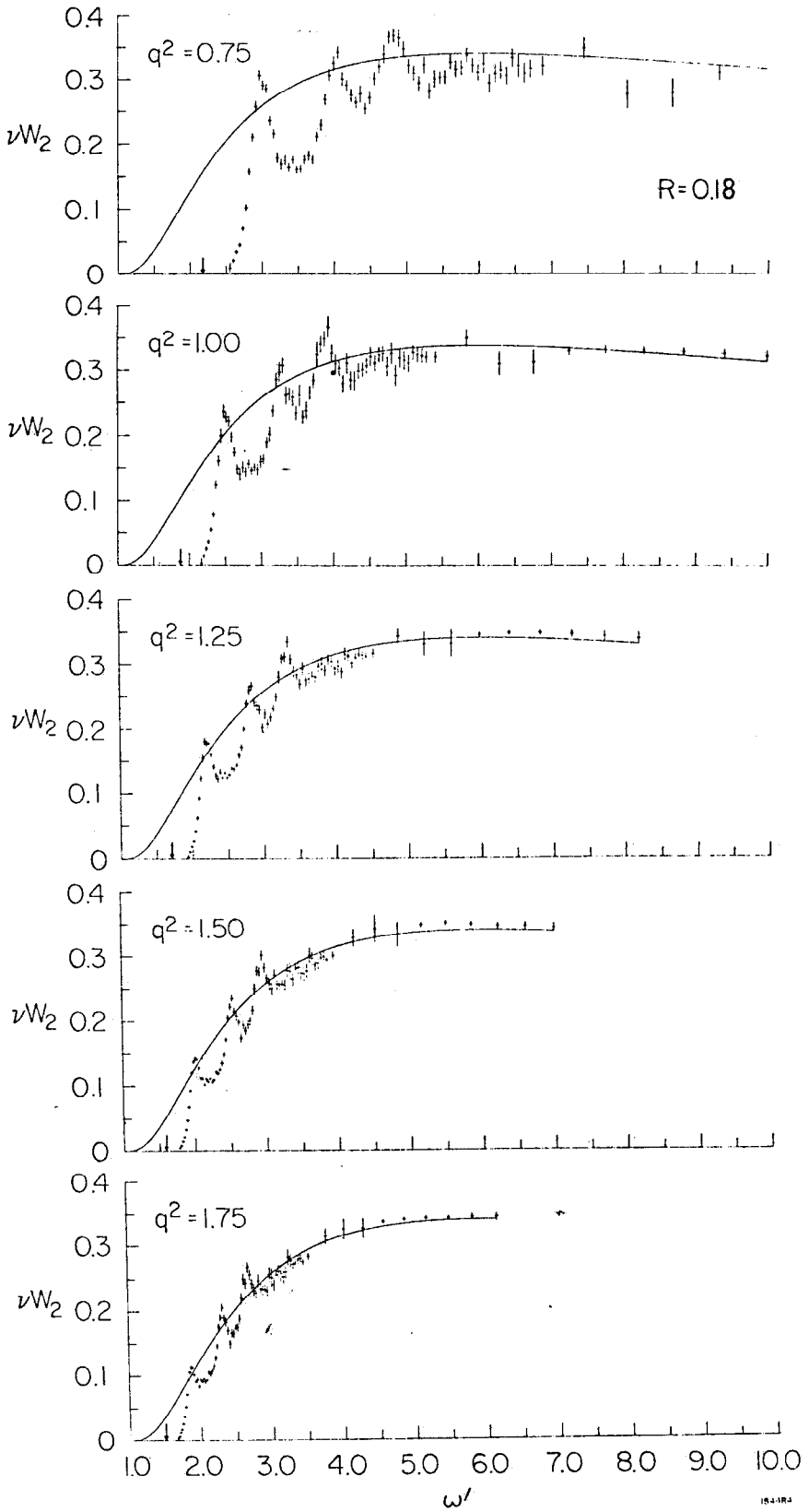
0.4
0.3
0.2
0.1
0
νW_2
$q^2 = 0.75$
R = 0.18
$q^2 = 1.00$
$q^2 = 1.25$
$q^2 = 1.50$
$q^2 = 1.75$
1.0
2.0
3.0
4.0
5.0
6.0
7.0
8.0
9.0
10.0
ω'

Fig. 3

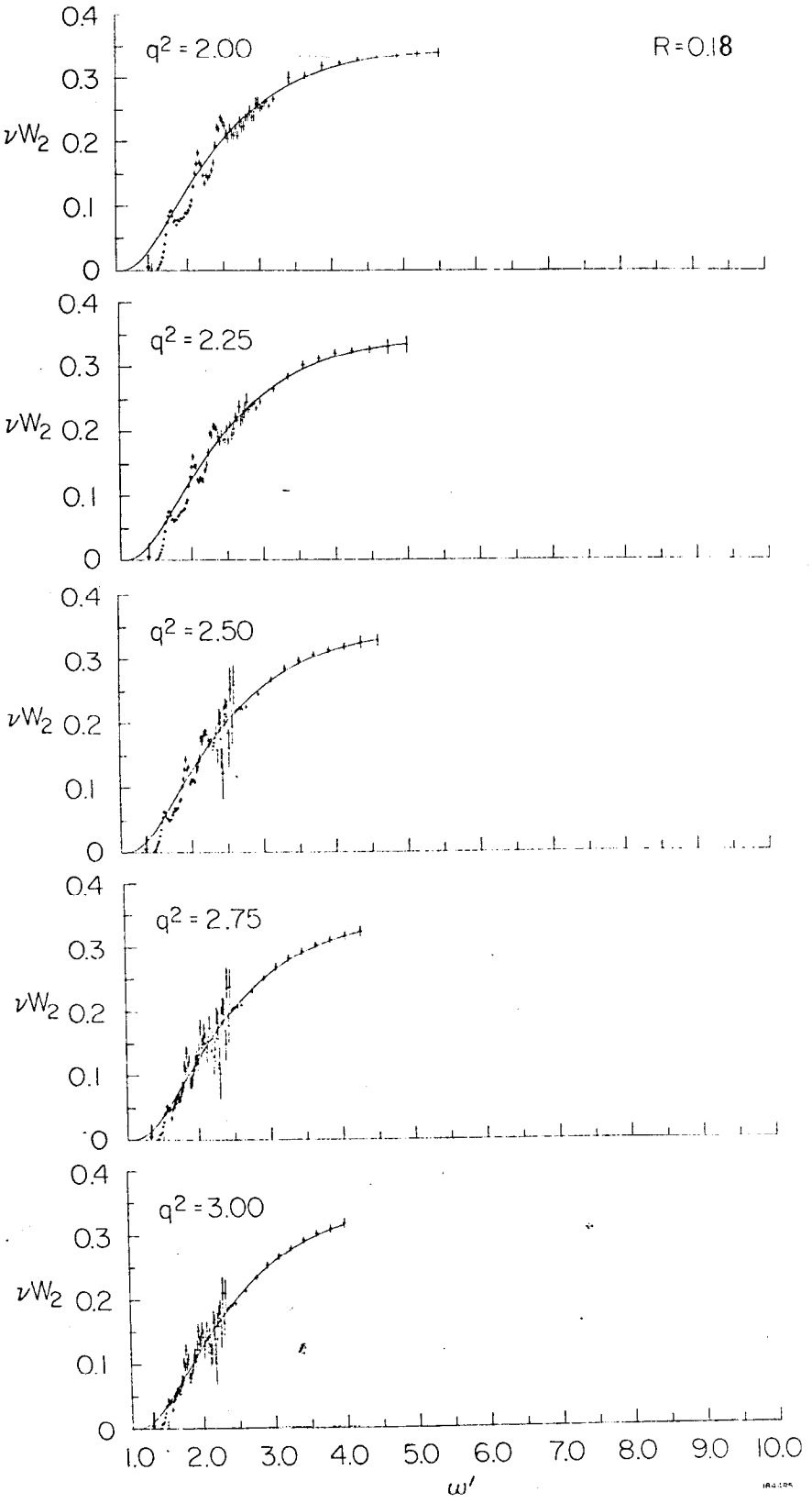
$q^2 = 2.00$
R = 0.18
$q^2 = 2.25$
$q^2 = 2.50$
$q^2 = 2.75$
$q^2 = 3.00$
νW_2
0.4
0.3
0.2
0.1
0
1.0
2.0
3.0
4.0
5.0
6.0
7.0
8.0
9.0
10.0
ω'

Fig. 4

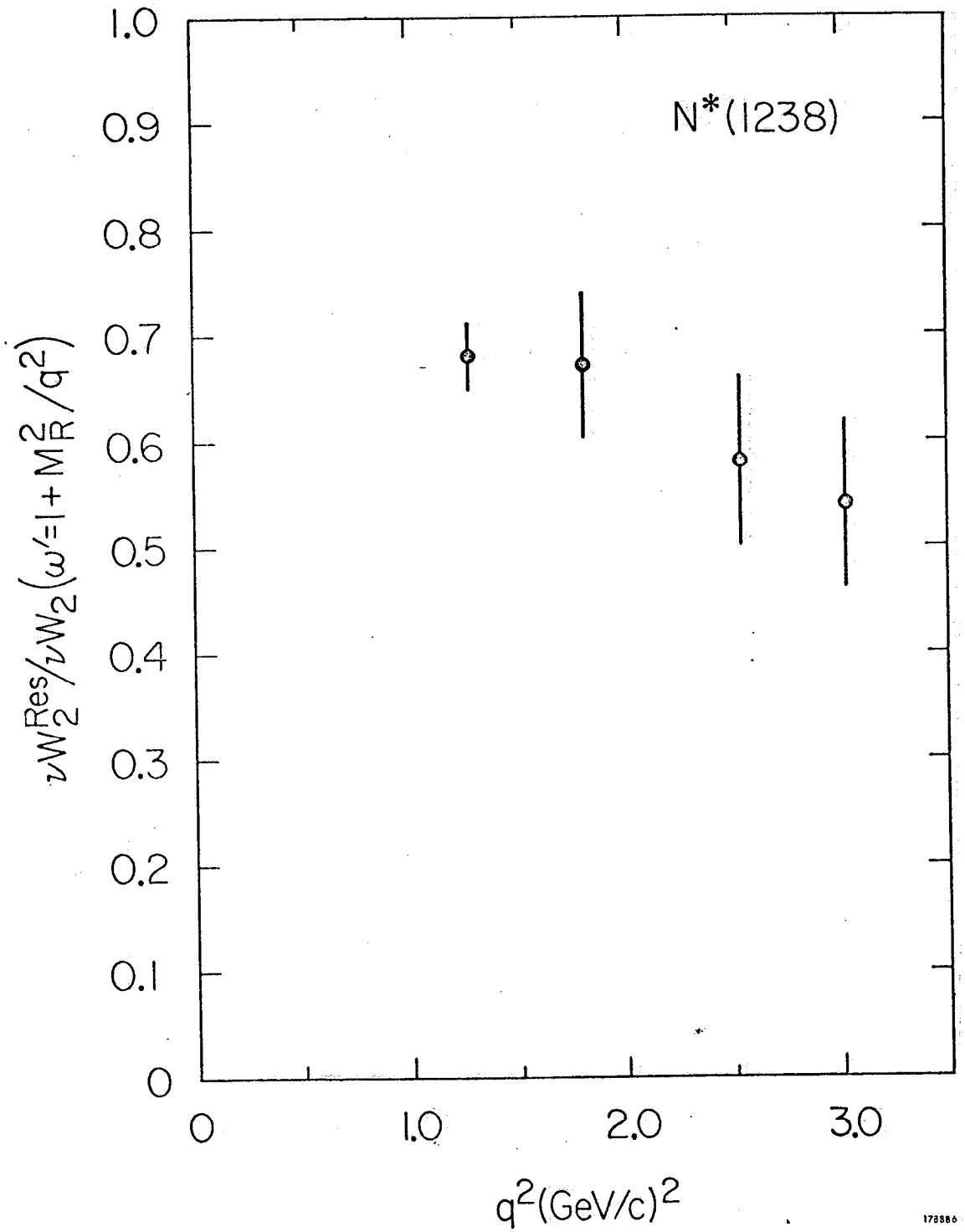
N*(1238)
$\nu W_2^{Res}/\nu W_2(\omega'=1+M_R^2/q^2)$
q^2(GeV/c)^2
1.0
0.9
0.8
0.7
0.6
0.5
0.4
0.3
0.2
0.1
0
0
1.0
2.0
3.0
178886

Fig. 5

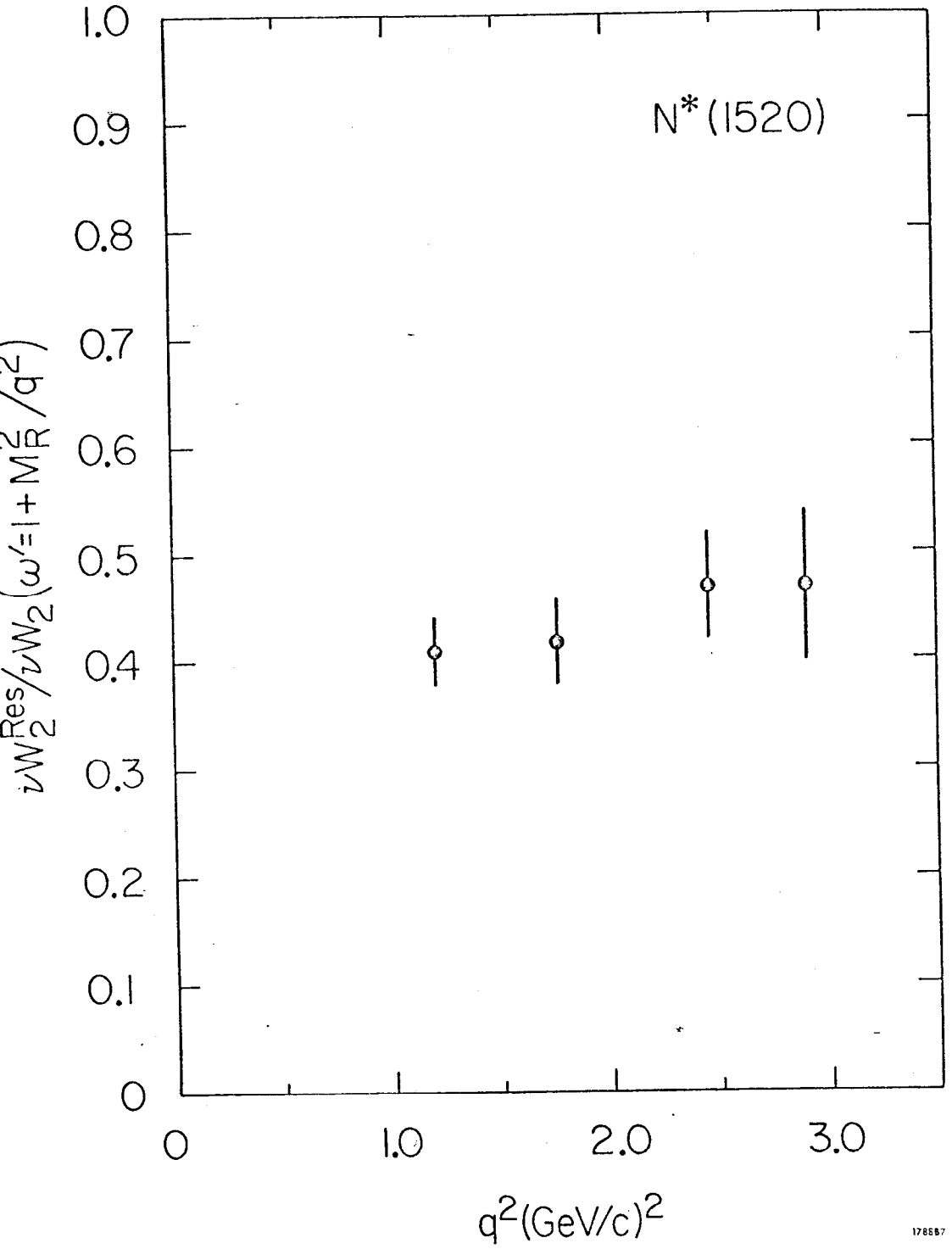
N*(1520)
1.0
0.9
0.8
0.7
0.6
0.5
0.4
0.3
0.2
0.1
0
0
1.0
2.0
3.0
$\nu W_2^{Res}/\nu W_2(\omega'=1+M_R^2/q^2)$
$q^2(GeV/c)^2$
178557

Fig. 6

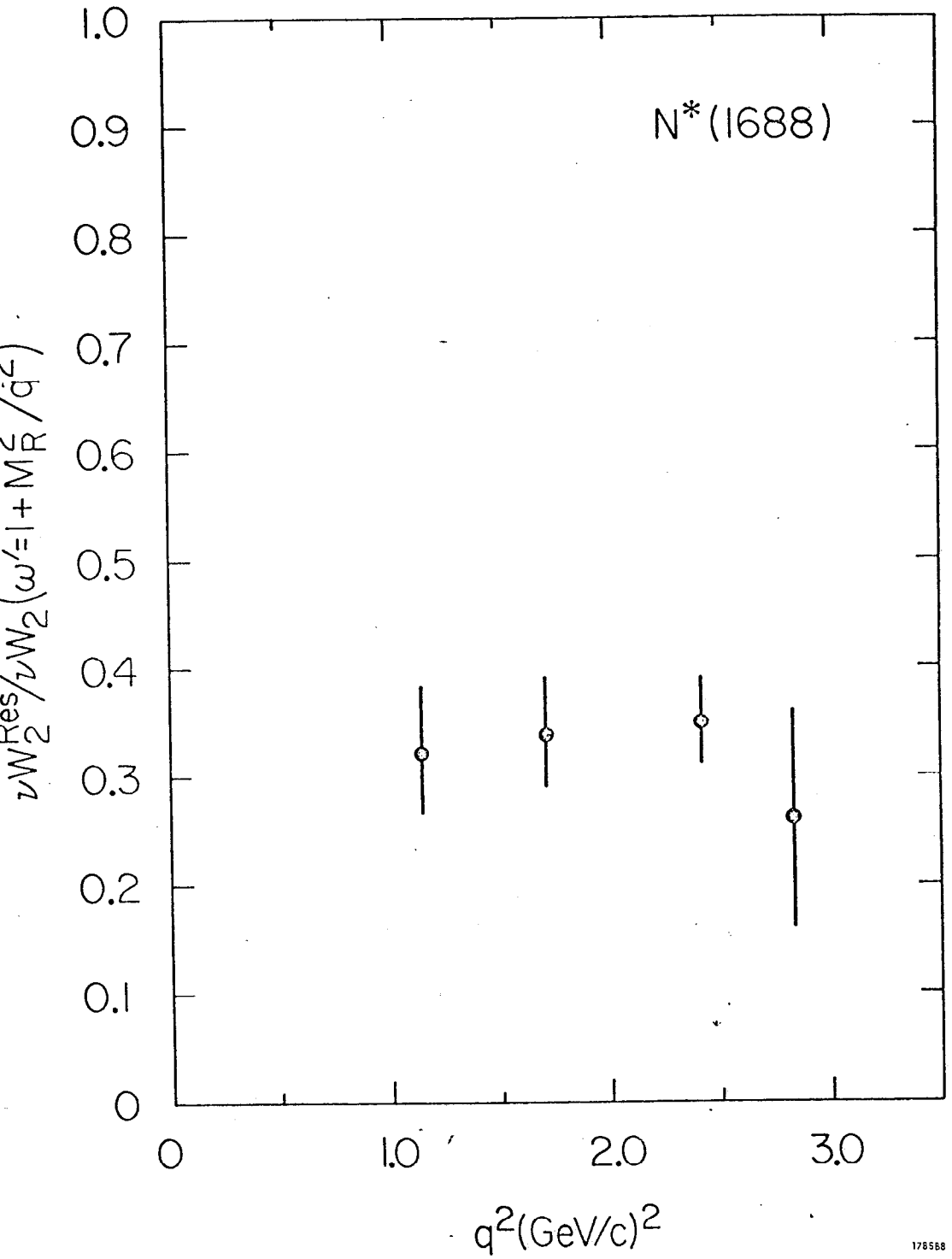
N*(1688)
$\nu W_2^{Res}/\nu W_2(\omega'=1+M_R^2/q^2)$
$q^2(GeV/c)^2$
1.0
0.9
0.8
0.7
0.6
0.5
0.4
0.3
0.2
0.1
0
0
1.0
2.0
3.0
178588

Fig. 7

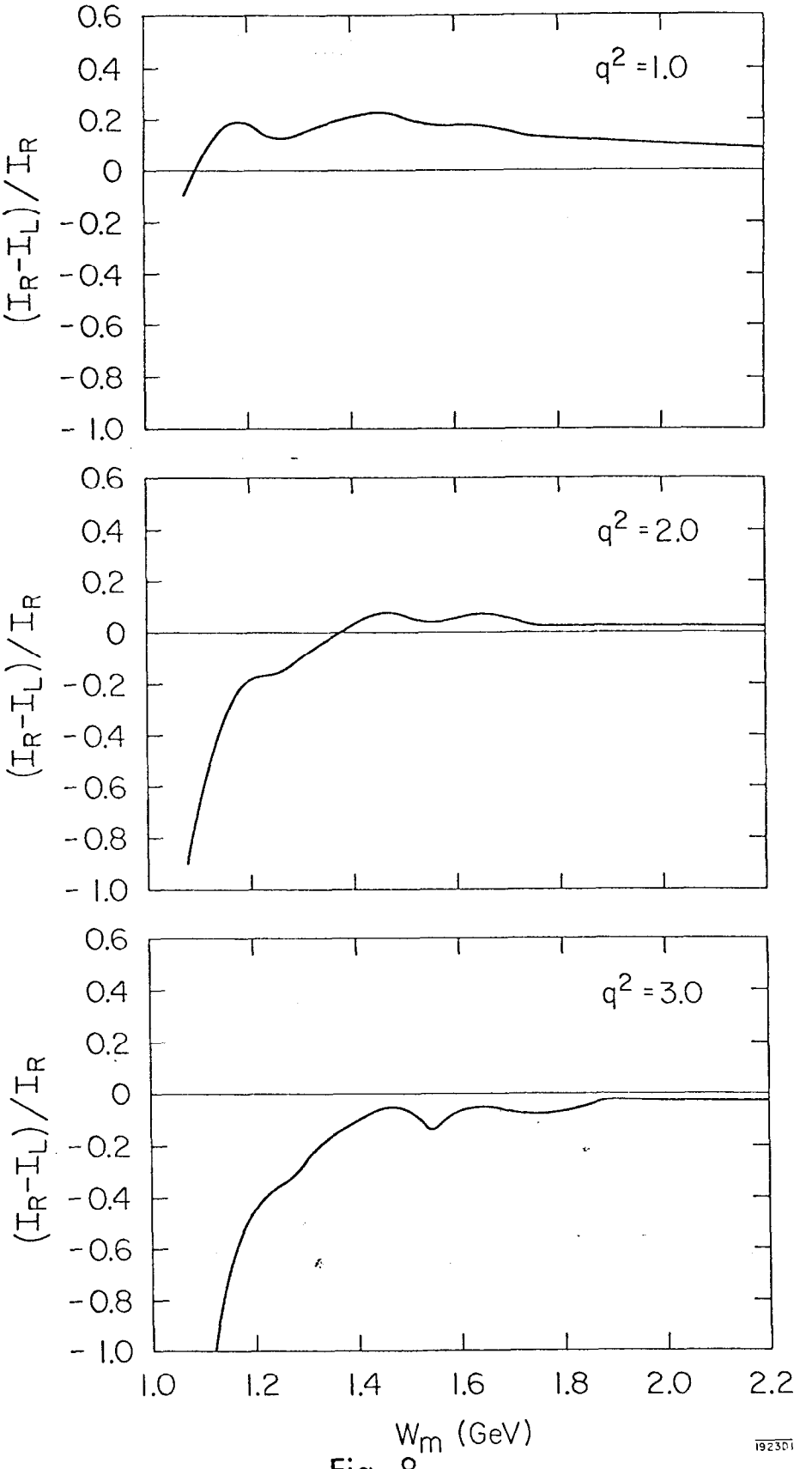
0.6
0.4
0.2
0
-0.2
-0.4
-0.6
-0.8
-1.0
$(I_R-I_L)/I_R$
$q^2 = 1.0$
$q^2 = 2.0$
$q^2 = 3.0$
1.0
1.2
1.4
1.6
1.8
2.0
2.2
W_m (GeV)
192301

Fig. 8

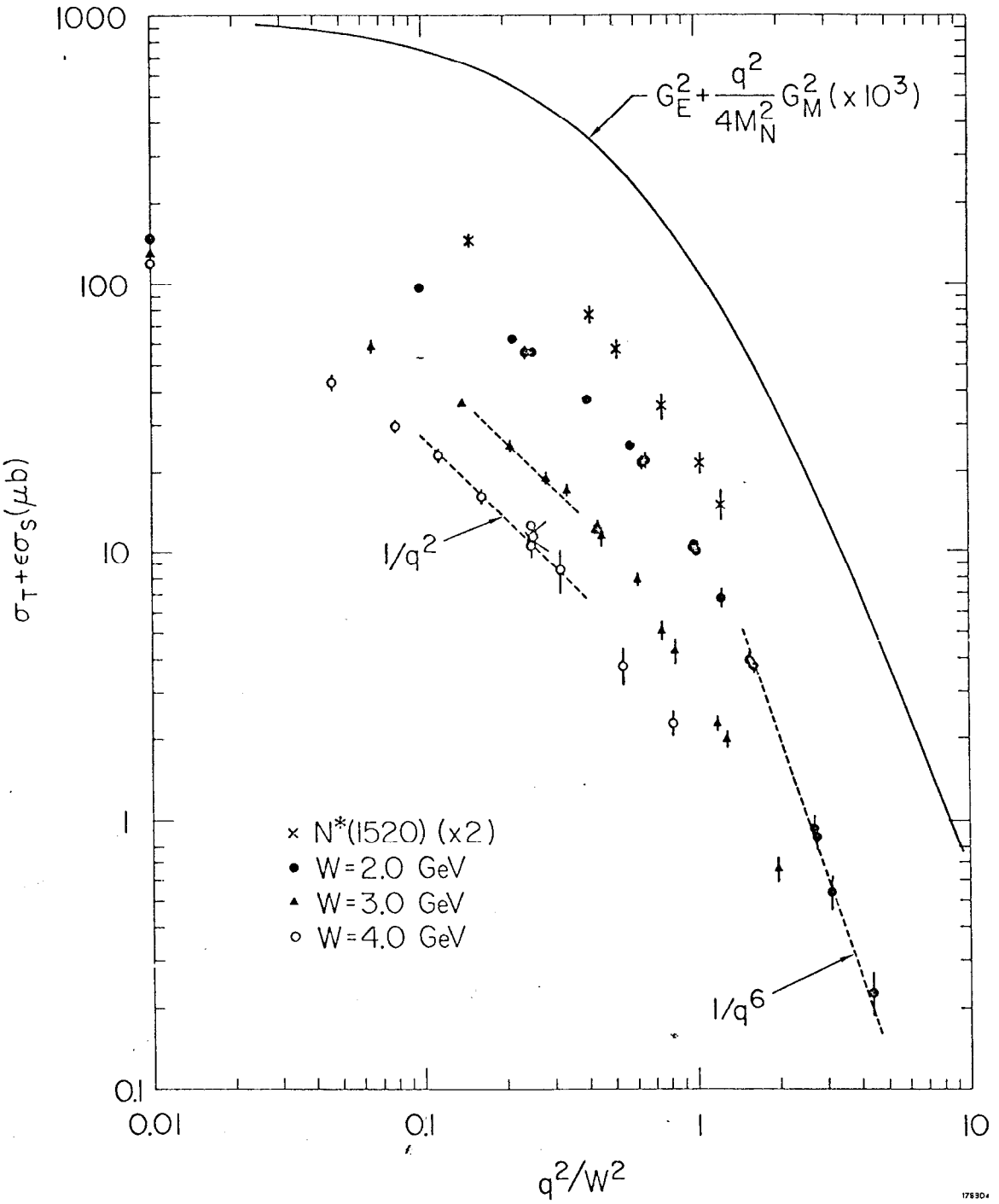
1000
100
10
1
0.1
0.01
0.1
1
10
$G_E^2 + \frac{q^2}{4M_N^2} G_M^2 (\times 10^3)$
$1/q^2$
$1/q^6$
× N*(1520) (x2)
• W=2.0 GeV
▲ W=3.0 GeV
○ W=4.0 GeV
$\sigma_T + \epsilon\sigma_S (\mu b)$
q^2/W^2
176304

Fig. 9

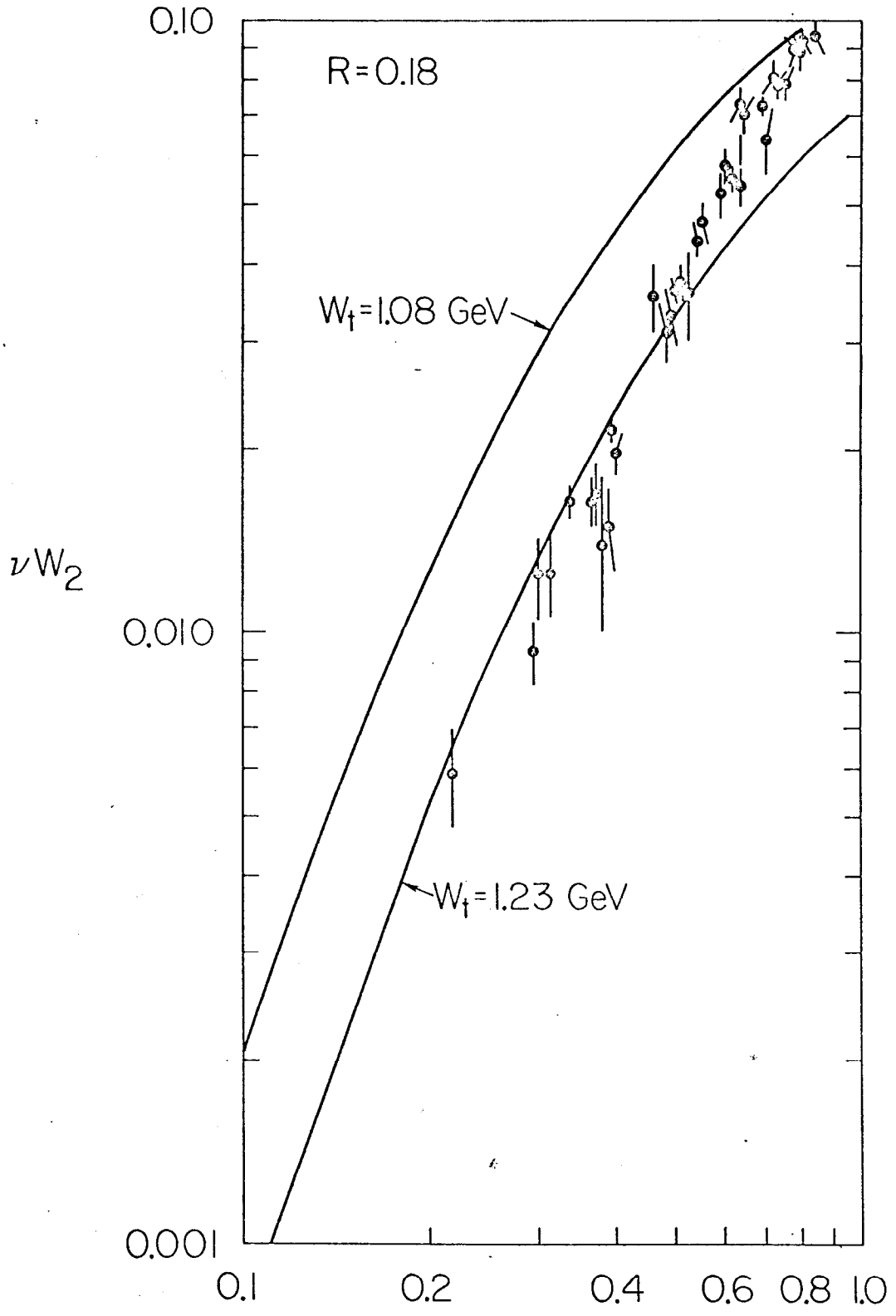
0.10
R=0.18
W_t=1.08 GeV
νW_2
0.010
W_t=1.23 GeV
0.001
0.1
0.2
0.4
0.6
0.8
1.0
$\omega'-1$
1788C15

Fig. 10

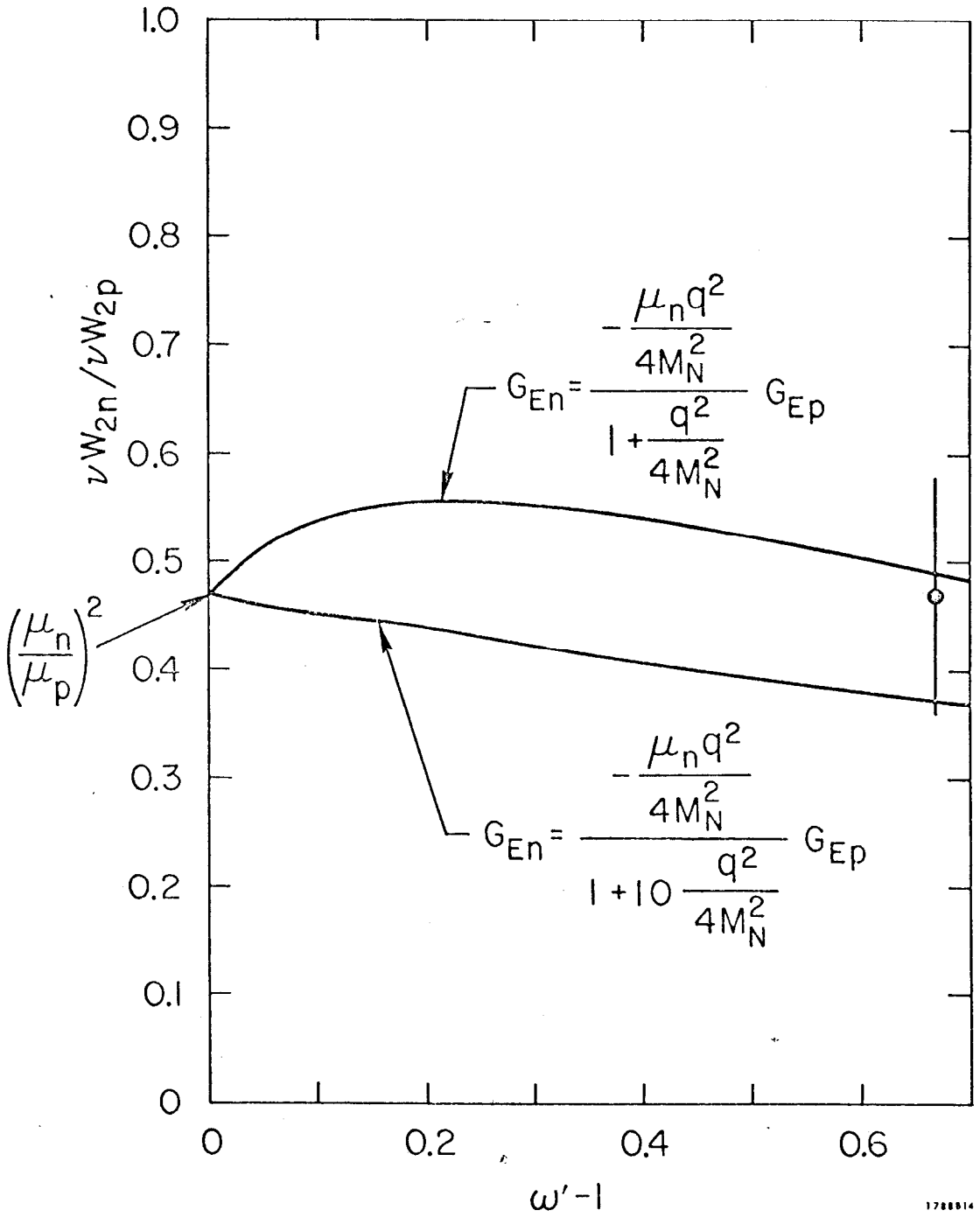
1.0
0.9
0.8
0.7
0.6
0.5
0.4
0.3
0.2
0.1
0
0
0.2
0.4
0.6
$\omega' - 1$
$\nu W_{2n} / \nu W_{2p}$
$\left(\frac{\mu_n}{\mu_p}\right)^2$
$G_{En} = \frac{-\frac{\mu_n q^2}{4M_N^2}}{1 + \frac{q^2}{4M_N^2}} G_{Ep}$
$G_{En} = \frac{-\frac{\mu_n q^2}{4M_N^2}}{1 + 10\frac{q^2}{4M_N^2}} G_{Ep}$
1788814

Fig. 11